ORGANOMETALLICS

Article

pubs.acs.org/Organometallics

# The Challenge of Palladium-Catalyzed Aromatic Azidocarbonylation: From Mechanistic and Catalyst Deactivation Studies to a Highly Efficient Process

Fedor M. Miloserdov,[†] Claire L. McMullin,[‡] Marta Martínez Belmonte,[†] Jordi Benet-Buchholz,[†] Vladimir I. Bakhmutov,[§] Stuart A. Macgregor,*[,‡] and Vladimir V. Grushin*[,†]

[†]Institute of Chemical Research of Catalonia (ICIQ), Tarragona 43007, Spain

[‡]Institute of Chemical Sciences, Heriot-Watt University, Edinburgh EH14 4AS, U.K.

[§]Department of Chemistry, Texas A&M University, College Station, Texas 77842, United States

*Supporting Information*

**ABSTRACT:** Azidocarbonylation of iodoarenes with CO and $NaN_3$, a novel Heck-type carbonylation reaction, readily occurs in an organic solvent−$H_2O$ biphasic system to furnish aroyl azides at room temperature and 1 atm. The reaction is catalyzed by Xantphos-Pd and exhibits high functional group tolerance. The catalyst deactivation product, [(Xantphos)-$PdI_2$], can be reduced in situ with PMHS to Pd(0) to regain catalytic activity. In this way, the catalyst loading has been lowered to 0.2% without any losses in selectivity at nearly 100% conversion to synthesize a series of aroyl azides in 80−90% isolated yield on a gram scale. Alternatively, the $ArCON_3$ product can be used without isolation for further transformations in situ, e.g., to isocyanates, ureas, benzamides, and iminophosphoranes. A detailed experimental and computational study has identified two main reaction pathways for the reaction. For both routes, Ar−I oxidative addition to Pd(0) is the rate-determining step. In the presence of CO in excess, the Ar−I bond is activated by the less electron-rich Pd center of a mixed carbonyl phosphine complex. Under CO-deficient conditions, a slightly lower energy barrier pathway is followed that involves Ar−I oxidative addition to a more reactive carbonyl-free (Xantphos)$Pd^0$ species. Mass transfer in the triphasic liquid−liquid−gas system employed for the reaction plays an important role in the competition between these two reaction channels, uniformly leading to a common aroyl azido intermediate that undergoes exceedingly facile $ArCO-N_3$ reductive elimination. Safety aspects of the method have been investigated.

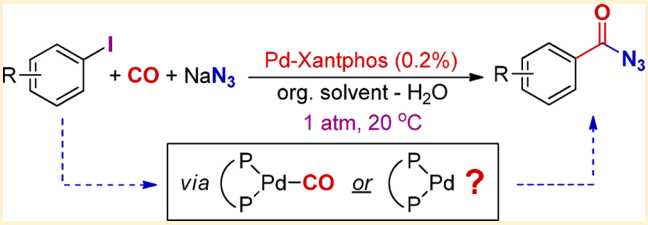


## INTRODUCTION

In 1974, Schoenberg and Heck[1] reported their groundbreaking discovery of Pd-catalyzed carbonylation of haloarenes (eq 1; e.g., X = I, Br and Nu = OR, $NR_2$). Since then, this reaction has become one of the most powerful tools for the synthesis of aromatic carbonyl compounds in both laboratory and industrial settings.[2] A broad variety of nucleophiles have been successfully employed in this transformation to furnish a diversity of products.

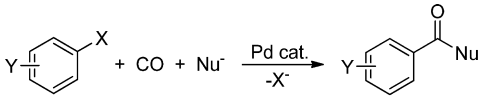


(1)

X = I, Br, Cl, OTf, etc.; $Nu^-$ = $OH^-$, $RO^-$, $NR_2^-$, etc.

Considering the vast research effort made by numerous groups working in the area,[2] it might be surprising that the Pd-catalyzed carbonylation methodology has not been applied to the synthesis of azidocarbonyl aromatic compounds $ArCON_3$ ($Nu^-$ = $N_3^-$ in eq 1). Aroyl azides are valuable intermediates and building blocks in the preparation of various useful compounds[3] such as isocyanates, amides, iminophosphoranes, and oxazoles.[4] Conventional routes to aroyl azides include diazotization of hydrazides and azidation of acid chlorides, mixed anhydrides, and N-acyl benzotriazoles with $NaN_3$.[3,5] These synthetic methods employ highly reactive and hazardous chemicals that limit their scope and functional group compatibility. Since methodologically new, high functional group tolerance routes to aroyl azides are certainly in demand, the following question arises: why is it that Pd-catalyzed aromatic azidocarbonylation (eq 1, where $Nu^-$ = $N_3^-$) has not been developed?

Upon superficial consideration, there should be no fundamental difference between azide and other nucleophiles that have been successfully used in the carbonylation reactions of haloarenes (eq 1). In-depth analysis of the literature data on aroyl azides and mechanisms of palladium catalysis suggests, however, that the development of Pd-catalyzed aromatic azidocarbonylation should be extremely challenging, if not impossible. In particular:

**Received:** November 20, 2013

  

**Scheme 1**

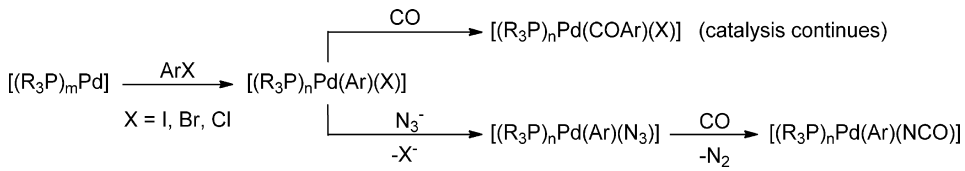


(1) A key step in the catalytic loop governing the carbonylation reaction (eq 1) is migratory insertion of CO into the Pd−C bond of $[(R_3P)_2Pd(Ar)(X)]$, the intermediate that is produced in the preceding step of ArX substrate oxidative addition to $R_3P$-stabilized Pd(0).[6] For X = I, Br, Cl, this reaction usually occurs easily and cleanly at 20−70 °C and atmospheric pressure (Scheme 1). In sharp contrast, complexes of the type *trans*-$[(R_3P)_2Pd(Ph)N_3]$ (R = Me, Et) do not undergo CO insertion into the Pd−Ph bond but are rather converted to *trans*-$[(R_3P)_2Pd(Ph)NCO]$ with concomitant release of $N_2$ under similar conditions (room temperature, 1 atm of CO),[7] as shown in Scheme 1.

(2) Being thermally stable, carboxylic acid derivatives (salts, esters, amides, etc.) formed in the carbonylation reactions (eq 1) easily survive the elevated temperatures that are needed for the process to occur. In sharp contrast, aroyl azides are thermally unstable compounds that rapidly undergo the Curtius rearrangement (Scheme 2) at such temperatures (80 °C and above).

**Scheme 2**

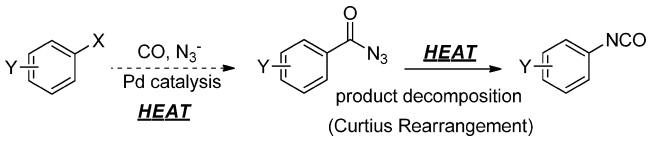


(3) The anticipated product, $ArCON_3$, is not only thermally unstable but also highly reactive toward tertiary phosphines that are used as stabilizing ligands for Pd catalysts employed in carbonylation and other coupling reactions. The facile Staudinger reaction[8] of the $ArCON_3$ produced with the reversibly dissociated $PR_3$ ligand would lead to immediate catalyst deactivation from the quick and irreversible formation of the corresponding phosphinimine $ArC(O)N{=}PR_3$ (Scheme 3).

**Scheme 3**

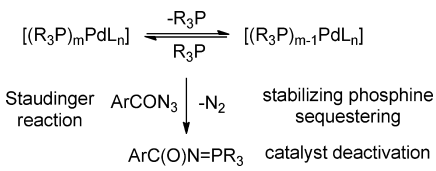


The three reactivity patterns described above and shown in Schemes 1−3 cast serious doubts on the very possibility of Pd-catalyzed aromatic azidocarbonylation. Nonetheless, herein we report that this transformation is not only possible, but can be highly efficient with a carefully designed and thoroughly studied catalytic system. In a preliminary communication,[9] we described the formation of aroyl azides from aryl iodides, CO, and $NaN_3$ in the presence of a Pd catalyst (2 mol %). Herein we report our most recent investigations into catalyst deactivation, which have led to the development of a practical and robust azidocarbonylation process on a gram scale with a Pd catalyst loading of only 0.2 mol %. We have also performed a number of tests to prove that the process is safe to run. Finally, our combined experimental and computational studies have uncovered novel and unique mechanistic features that are characteristic not only of the current process but also of other Heck-type[1] carbonylations. It is apt to note that, surprisingly, there have been no reports of detailed studies of the mechanism of palladium catalysis of carbonylative reactions of aryl halides in general and Ar−X oxidative addition to Pd(0) in the presence of CO in particular.

## ■ EXPERIMENTAL STUDIES

**Early Studies.** Originally, we intended to develop the Pd-catalyzed synthesis of aryl azides from the corresponding haloarenes and an inorganic azide source such as $NaN_3$ (Scheme 4). Previous attempts to perform this transformation have been unsuccessful, although Pd-catalyzed azidation of vinylic bromides to give 1*H*-1,2,3-triazoles has been reported.[10] As both oxidative addition of ArX to Pd(0) and halide/azide metathesis reactions of Pd(II) complexes[7,11] are well-known, we reasoned that it is the Ar−$N_3$ reductive elimination from Pd(II) that must be the problematic step of the process (Scheme 4).

**Scheme 4**

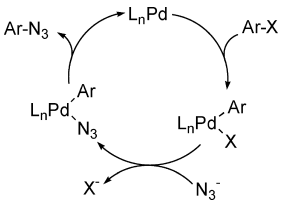


To study Ar−$N_3$ reductive elimination from Pd(II), the product-forming step in the proposed catalytic loop, we prepared $[(Ph_3P)_2Pd(Ph)(N_3)]$ from $[(Ph_3P)_2Pd(Ph)(Br)]$ and $NaN_3$. This complex was found to be exclusively trans both in solution ($^1$H and $^{31}$P NMR) and in the solid state (X-ray diffraction). Interestingly, $[(Ph_3P)_2Pd(Ph)(N_3)]$ was found to crystallize in two polymorphic forms displaying either a staggered or an eclipsed conformation along the P−Pd−P axis (Figures 1 and 2).

The new azido complex *trans*-$[(Ph_3P)_2Pd(Ph)(N_3)]$ appeared to be unexpectedly thermally stable, exhibiting no sign of decomposition at 80−100 °C in benzene or toluene for 15−24 h. At 135 °C in xylenes, however, $[(Ph_3P)_2Pd(Ph)(N_3)]$ decomposed to give mostly $Ph_2$ and $PhN{=}PPh_3$ (GC-MS). The iminophosphorane was evidently produced by the Staudinger reaction[8] of the transient $PhN_3$ with the $PPh_3$ ligand. Attempts to perform this reaction catalytically, i.e. in the presence of excess $PPh_3$, were unsuccessful. Importantly,

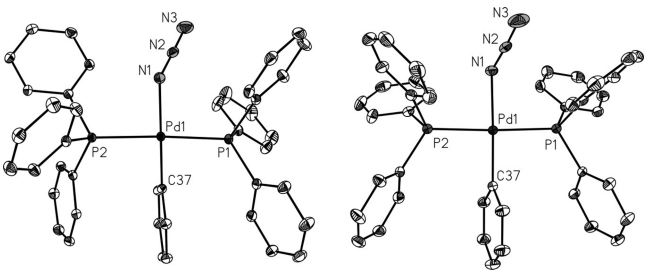


**Figure 1.** ORTEP drawings of the staggered (left) and eclipsed (right) conformers of *trans*-[$(Ph_3P)_2Pd(Ph)(N_3)$] with all H atoms omitted and thermal ellipsoids drawn at the 50% probability level.

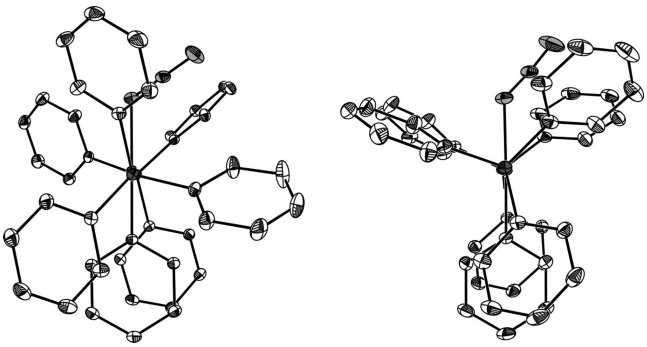

**Figure 2.** ORTEP views of the staggered (left) and eclipsed (right) conformers of *trans*-[$(Ph_3P)_2Pd(Ph)(N_3)$] along the P−Pd−P axis with all H atoms omitted and thermal ellipsoids drawn at the 50% probability level.

during these studies we found that bubbling CO through a solution of [$(Ph_3P)_2Pd(Ph)(N_3)$] containing PhI and $PPh_3$ in benzene at 50 °C triggered a clean transformation to [$(Ph_3P)_2Pd(COPh)I$][6] and $PhC(O)N{=}PPh_3$[12] ($^{31}P$ NMR). The formation of the latter indicated that $PhCON_3$ was formed as an intermediate that was scavenged with $PPh_3$ in the Staudinger reaction. These observations prompted our search for a Pd catalyst for the synthesis of aroyl azides directly from ArI, CO, and $N_3^-$.

**Catalyst Screening.** A large series of scouting experiments resulted in the identification of Xantphos-stabilized Pd complexes as active catalysts for the reaction of iodobenzene with CO and $NaN_3$ to give benzoyl azide (eq 2). Of numerous ligands ($Ph_3P$, *o*-$Tol_3P$, $Cy_3P$, *t*-$Bu_3P$, dppe, dppp, dppb, dppf, *rac*-BINAP, Xantphos, *i*-Pr-Xantphos, *t*-Bu-Xantphos, and DPEphos) screened in combination with $Pd(OAc)_2$ or $Pd_2(dba)_5$[13] precursors, only Xantphos[14,15] gave rise to an active catalyst.[9] With the other ligands, the yield of $PhCON_3$ from PhI never exceeded 6% under a variety of conditions.[16] The highest activity was observed for a 1:1 Pd(0) to Xantphos molar ratio, in accord with the literature data.[17]

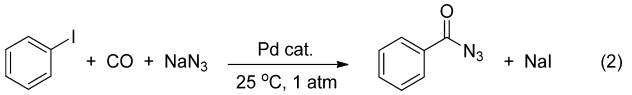


(2)

**The Need for Full Conversion: Performing the Reaction under Biphasic Conditions.** In most instances, the aroyl azide product and the iodoarene starting material exhibited close $R_f$ parameters and therefore could not be efficiently separated by column chromatography. This observation dictated the need for driving the azidocarbonylation reaction to full conversion, so that the product could be isolated pure. It was found ($^{19}F$ NMR) that nearly quantitative conversions of 4-$FC_6H_4I$ could be obtained by running the reaction in the presence of water, especially under biphasic conditions. In THF−$H_2O$, the reaction stalled after quickly reaching 80−90% conversion, likely because of catalyst deactivation with the iodide[18,19] released in the transformation (eq 2). Performing the reaction in a water−organic solvent biphasic system effectively eliminated the inhibiting effect of iodide that accumulated in the aqueous layer, whereas the active Pd catalyst remained in the water-immiscible organic phase. In $H_2O$−benzene or $H_2O$−toluene, the reaction afforded 4-$FC_6H_4CON_3$ in 97% yield at >99% conversion with 2% Pd. However, benzene is toxic and the boiling point of toluene (110 °C) prevents isolation of the volatile and thermally sensitive benzoyl azide product. As a result of a series of experiments, it was found that the aromatic organic phase can be successfully substituted with a 2:1 v/v nontoxic, low-boiling mixture of THF and hexane. Although high conversions (>90%) and yields of up to 88% could be obtained under such conditions with only 1% Pd, we settled on 2 mol % of the catalyst in order to reach full conversion that is critical for isolation of the product in pure form. A summary of the optimization studies described above can be found in Table 2 of the Supporting Information to the preliminary communication.[9]

**Azidocarbonylation of Substituted Aryl Iodides.** Having optimized the reaction (eq 2) under biphasic conditions, we performed the azidocarbonylation on a series of aryl iodides (Table 1).[9] The reactions smoothly proceeded at 23−50 °C and atmospheric pressure of CO. Quantitative conversions were achieved for all of the substrates **1a−r**, allowing isolation of the pure aroyl azide products **2a−r** in high yield. Various functional groups were tolerated and the reaction proceeded smoothly and selectively with substrates bearing electron-withdrawing (**2e−l,p**) and electron-donating (**2b−d,n**) substituents on the ring. Likewise, heteroaryl iodides, 2-iodothiophene (**1q**) and 3-iodopyridine (**1r**), were cleanly converted to **2q** and **2r** in 87% and 75% isolated yields, respectively. The reaction of 2-iodopyridine, however, gave rise to a mixture of products (2-PyNCO, 2-$PyCONH_2$, and 2-$PyNH_2$) under similar conditions, evidently because of the low thermal stability of 2-$PyCON_3$[20] and possibly catalyst modification via the previously documented[21] dimerization of 2-pyridyl Pd complexes via the N atoms of the Py ring.

With ortho-substituted aryl iodide substrates, the reaction did not produce aroyl azides but rather gave amides, amines, and diarylureas.[9] A mixture of all three was formed in the reaction of 2-iodotoluene. 2-Iodoanisole and 1-iodonaphthalene reacted more selectively to give predominantly ureas. In this way, *N,N′*-bis(1-naphthyl)urea (**3a**; 76% yield) and *N,N′*-bis(2-methoxyphenyl)urea (**3b**; 74% yield) were isolated from the reactions of 1-iodonaphthalene and 2-iodoanisole, respectively. Considering the fact that ortho-substituted $ArCON_3$ are 50−200 times less stable toward the Curtius rearrangement than their meta and para isomers,[20,22] the different reaction outcome for iodoarenes bearing an ortho substituent is hardly surprising. The steric bulk of a group in the ortho position weakens the conjugation between the aromatic ring and the $CON_3$ function, thereby destabilizing the latter and lowering the barrier to the Curtius rearrangement. As a result, ortho-substituted aroyl azides formed in the reaction quickly rearrange to the corresponding isocyanates. Conversion of the latter to an

**Table 1. Pd-Catalyzed Azidocarbonylation of Iodoarenes**[a]

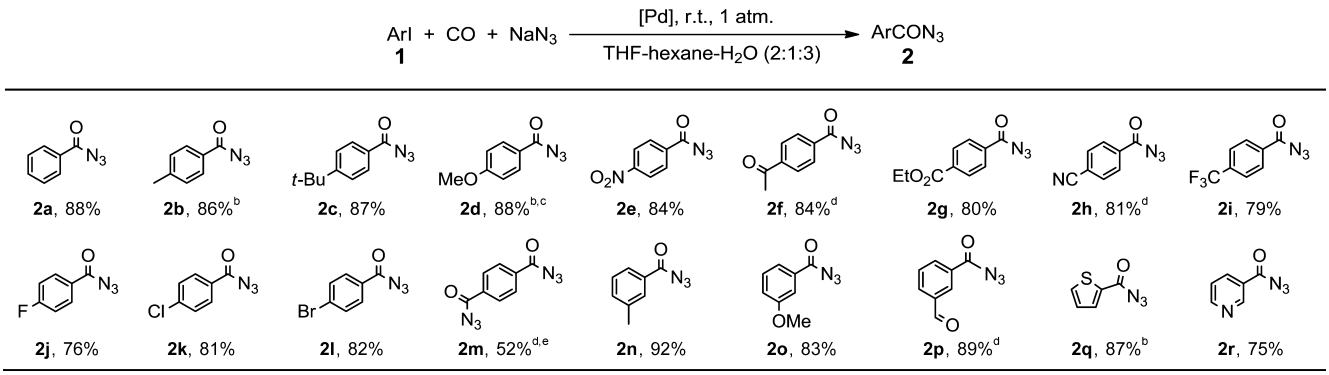


[a]Reaction conditions: ArI (1 mmol), $NaN_3$ (1.2 mmol), $Pd_2(dba)_5$[13] (0.01 mmol; 2 mol % Pd), Xantphos (2 mol %) in THF (2 mL), hexane (1 mL), and water (3 mL). [b]50 °C (oil bath). [c]Isolated product contained ca. 2% of $PhCON_3$ as a result of P−Ar/Pd−Ar′ exchange. [d]Isolated product contained dba. [e]With 1 mmol of 1,4-diiodobenzene (**1m**) and double amounts of all reagents and solvents.

aniline under the reaction conditions, followed by its addition to the as yet unreacted isocyanate, gives the urea (Scheme 5).

**In Situ Modification of Catalytically Produced Aroyl Azides.** As mentioned above, aroyl azides are reactive compounds that can be used in a variety of useful transformations. We were able to demonstrate that some of these transformations could be conveniently carried out in situ, without isolation of the aroyl azide product formed in the catalytic process (Scheme 6).[9] The substrate of choice was 4-

**Scheme 5**

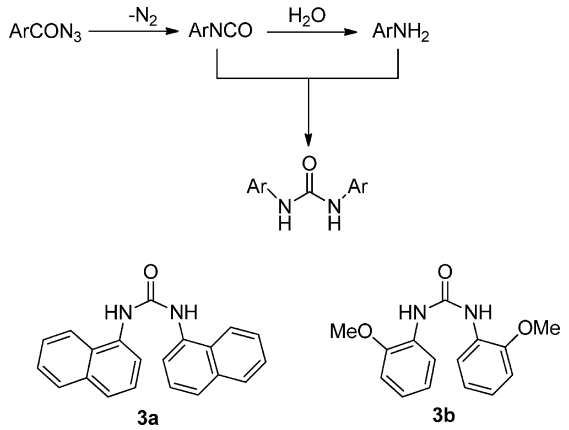


fluoroiodobenzene (**1j**), so that the transformations could be conveniently monitored by $^{19}F$ NMR. Conducting the azidocarbonylation of **1j** in the presence of polymethylhydrosiloxane (PMHS; 2 equiv) at 50 °C gave rise to 4-fluorobenzamide (**4**) in nearly quantitative yield. It is worth noting that catalytic carbonylation of aryl halides to primary benzamides represents a considerable challenge.[23] In another experiment, the entire reaction mixture containing freshly produced **2j** was treated with $PPh_3$ (1.1 equiv) to prompt the Staudinger reaction that furnished iminophosphorane **5** in 85% overall yield. Furthermore, performing the azidocarbonylation in toluene−water provided a convenient means to carry out the Curtius rearrangement by simply separating and heating the toluene phase containing the $ArCON_3$ product. In this way, 4-fluorophenyl isocyanate (**6**) was obtained in 86% yield (Scheme 6), as calculated from the amount of **1j** used. Aryl isocyanates[24] are widely used in the production of a broad variety of polymers, materials, and valuable chemicals, including

**Scheme 6**

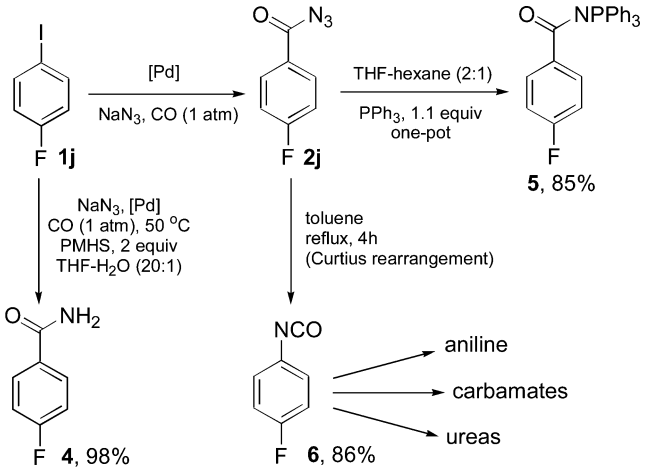


carbamates, anilines, and ureas. Examples of the synthesis of aromatic isocyanates from the corresponding aryl halides are extremely rare. Tkatchenko et al.[25] have patented Ni-catalyzed reaction of haloarenes with NaOCN to produce aryl isocyanates and their derivatives in up to 50% yield. Most recently, Buchwald's group[26] demonstrated direct Pd-catalyzed transformation of aryl chlorides and triflates to aryl isocyanates that were converted in situ to unsymmetrical ureas[26a] and carbamates.[26b]

**Catalyst Deactivation.** The identification and in-depth understanding of the side transformations resulting in catalyst deactivation can be a powerful tool for the design and development of efficient catalytic processes.[13b,27] We therefore studied the loss of catalytic activity in the azidocarbonylation reaction.

As mentioned above, attempts to lower the catalyst loading from 2% to 1% resulted in incomplete conversion. To gain insight into the loss of catalytic activity, we set up a reaction with a larger quantity of iodobenzene (10 mmol of PhI in 0.5 mL of THF) and a lower amount of the Xantphos-$Pd_2(dba)_5$ catalyst (0.2 mol % Pd). After 2 h under such conditions, the organic phase turned deep purple and the catalytic process stopped at ca. 65% conversion. The $^{31}P$ NMR spectrum of the organic phase displayed a broad resonance at 6.4 ppm that could not be assigned to any of the identified intermediates

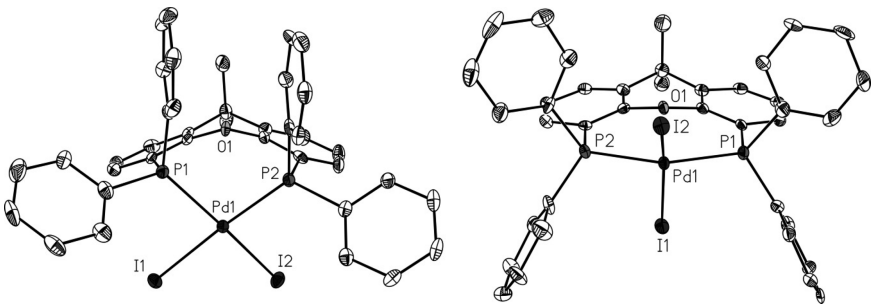


**Figure 3.** ORTEP drawing of *cis*-[(Xantphos)$PdI_2$]·$CH_2Cl_2$ (***cis*-7**·$CH_2Cl_2$, left) and *trans*-[(Xantphos)$PdI_2$] (***trans*-7**, right) with the $CH_2Cl_2$ molecule and all H atoms omitted and thermal ellipsoids drawn at the 50% probability level.

involved in the catalytic loop (see below). The dark purple color suggested that the signal at 6.4 ppm might be from [(Xantphos)$PdI_2$] (**7**). This assumption was probed by an independent synthesis of **7** from [(Xantphos)$PdCl_2$] (**8**) and NaI. Indeed, both the color and $^{31}$P NMR parameters displayed by the thus-prepared **7** (97% yield) appeared identical with those displayed by the catalyst deactivation product. Furthermore, spiking the reaction mixture after catalyst deactivation with an authentic sample of **7** resulted in growth in intensity of the $^{31}$P NMR signal at 6.4 ppm. We therefore concluded that the loss of catalytic activity should be attributed to gradual conversion of Pd species in the system to **7**. As was established by an independent run, **7** was indeed poorly catalytically active in the azidocarbonylation reaction.[28] As a new compound, **7** was fully characterized and found to exist as a mixture of cis and trans isomers both in solution and in the solid state (Figure 3). In solution, the cis to trans ratio was both solvent and temperature dependent. While only *trans*-**7** could be observed in benzene at room temperature, both the cis and trans isomers of **7** were detected in $CH_2Cl_2$ ($^{31}$P NMR). This trend is similar to the reported[29,30] behavior of [(Xantphos)-Pd(Ph)($CF_3$)]. Furthermore, the cis to trans ratios for **7** in $CH_2Cl_2$, as determined by $^{31}$P NMR, were 1:3.5 and 1:1.2 at 25 and −30 °C, respectively. Such solvent and temperature dependence of the cis to trans ratio for square-planar $d^8$ complexes is well-known.[31]

**Reactivation of the Poisoned Catalyst. Efficient Catalysis with 0.2% Pd.** While it is not entirely clear how **7** is formed during the catalytic process, the revealed catalyst deactivation pattern differs considerably from that previously established[27] for the related Pd-catalyzed aromatic cyanation. Importantly, unlike cyanide, azide is *not* capable of displacing the phosphine ligand on Pd(II) complexes involved in the transformation. Possible reaction pathways from the catalytically active Pd complexes discussed below to **7** might involve single electron transfer or redox processes. Although obviously occurring to a minor extent, these side reactions eventually lead to the formation of inactive **7** as the major Pd species in the reaction medium. Luckily, however, this catalyst deactivation does not involve structural changes to the phosphine ligand. Evidently, during the catalysis the P centers of Xantphos remain inaccessible to engage in the Staudinger reaction (Scheme 3) and are not oxidized in the Pd(II)/P(III) to Pd(0)/P(V) process.[32] We therefore reasoned that the catalytic activity could be recovered by reducing the poisoned catalyst in the form of [(Xantphos)$PdI_2$] (**7**) to Xantphos-stabilized Pd(0).

It was found that Zn dust and polymethylhydrosiloxane (PMHS) can both reduce **7** to Pd(0). Of the two, low-cost, stable, and environmentally friendly PMHS was not only more

**Table 2. Pd-Catalyzed Azidocarbonylation of Iodoarenes (10 mmol) in the Presence of 8 (0.2%) and PMHS[a]**

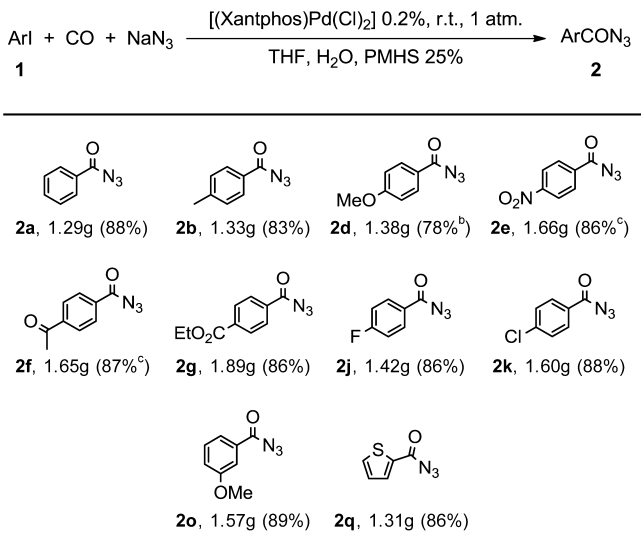


[a]All yields are isolated yields of pure products. Reaction conditions: ArI (10 mmol), $NaN_3$ (12 mmol), [(Xantphos)$PdCl_2$·$CH_2Cl_2$] (**8**; 0.02 mmol; 0.2 mol % Pd), $K_2CO_3$ (0.2 mmol; 2 mol %), in THF (0.5 mL) and water (2 mL) at 23 °C. [b]2 mL THF. [c]3 mL THF.

attractive but also showed superior performance. After a series of catalytic runs, it was established that, in the presence of 0.25 mol equiv of PMHS, iodobenzene can be azidocarbonylated at >99% conversion in 4−6 h with only 0.2% Pd.[33] Performing the reaction in the presence of PMHS also allowed the use of air-stable and easily accessible [(Xantphos)$PdCl_2$] (**8**) as added catalyst in place of the oxygen-sensitive Xantphos-$Pd_2$(dba)$_5$ system. In this way, **8** is reduced in situ with PMHS to give catalytically active Xantphos-ligated Pd(0). Another advantage of using **8** is the avoidance of the presence in the reaction of dba that might contaminate the aroyl azide product.[9] It was also taken into consideration that the reduction of [(Xantphos)-$PdCl_2$] with PMHS in the presence of water produces HCl that lowers the pH of the medium, thereby increasing the concentration of hazardous hydrazoic acid. Although HCl is generated in only minute quantities, 0.4% (2 equiv per **8** that is used in the amount of 0.2 mol %), we performed the catalytic reaction in the presence of $K_2CO_3$ (2%) to neutralize the HCl and thus prevent the formation of $HN_3$. Under the optimized new conditions, a series of aryl iodides were successfully converted to the corresponding aroyl azides with only 0.2 mol % of **8** (Table 2). These reactions were performed on a 10

mmol scale and furnished the corresponding pure products in 78−89% isolated yield.

Numerous attempts to efficiently azidocarbonylate less reactive bromoarenes were unsuccessful. While ligands, solvents, and temperature were varied in a broad range, the conversion never exceeded 5% even for more electrophilic, electron-deficient aryl bromides. At the elevated temperatures required for Ar−Br oxidative addition to Xantphos-stabilized Pd(0) to occur, the catalyst is quickly deactivated by the Staudinger reaction of the $ArCON_3$ product with the phosphine ligand. In the presence of CO, activation of bromoarenes with tertiary phosphine complexes of zerovalent palladium is even more sluggish and therefore even higher temperatures are needed (see below). Indeed, evidence has been reported[34,35] for the diminished reactivity of phosphine-ligated Pd(0) under CO pressure. This is in full accord with the fact that higher CO concentrations result in more efficient displacement of the phosphine ligands on the metal with $\pi$-acidic carbonyls, thereby lowering the reactivity of the Pd(0) center toward electrophiles.

**Safety.** The reactions summarized in Table 2 produced gram quantities of aroyl azides that were isolated and purified. As many azido derivatives are explosive, comments are due on the safety aspects of the developed catalytic azidocarbonylation method. The so-called "azidophobia" often originates from the extreme shock sensitivity of certain metal azides.[36] While care must be exercised when handling organic azides, some of them are less explosive than others and have been safely used on a large scale.[37] We have not experienced safety problems running the azidocarbonylation reactions and manipulating organic azide derivatives reported herein.

In this work, we dealt not only with organic azides but also with azido complexes of palladium. The simplest palladium azide, $[Pd(N_3)_2]$, is highly shock sensitive and explosive.[38] Tetraazidopalladates such as $[Pd(NH_3)_4]^{2+}[Pd(N_3)_4]^{2-}$ are detonated by friction or shock.[38b] On the other hand, nonhomoleptic Pd(II) azide derivatives bearing other ligands can be stable and nonexplosive, e.g., $[Py_2Pd(N_3)_2]$.[38b] All of the phosphine-ligated mono-azido organopalladium complexes prepared in this work were stable compounds that did not exhibit any signs of explosiveness. It was conceivable, however, that small quantities of diazido Pd(II) species could emerge in the catalytic process from metathesis reactions of the $NaN_3$ reagent with $[(Xantphos)PdI_2]$ (**7**, catalyst deactivation product) or $[(Xantphos)PdCl_2]$ (**8**, added catalyst). To assess the safety of such diazido species, we prepared $[(Xantphos)Pd(N_3)_2]$ (**9**) by reacting **8** with sodium azide in $CHCl_3-H_2O$ (94% yield). Complex **9** was fully characterized, including by single-crystal X-ray diffraction (Figure 4) and found to be stable. This diazide was not shock-sensitive (striking with a hammer) and did not show any signs of decomposition in DMF solution at 100 °C after 4 h. We conclude that Xantphos-stabilized azido palladium species involved in the catalytic process are safe compounds. One must bear in mind, however, that (i) in the presence of $NaN_3$ and in the absence of stabilizing tertiary phosphine or other ligands a Pd(II) source may be converted to highly explosive species such as $[Pd(N_3)_2]$[38] and (ii) azido derivatives should always be handled with care.

**Azidocarbonylation Mechanism.** Like all Pd-catalyzed cross-coupling reactions of aryl halides, the azidocarbonylation involves oxidative addition of the haloarene substrate to Pd(0) as the first key step. Oxidative addition of PhI to $Pd_2(dba)_3$/

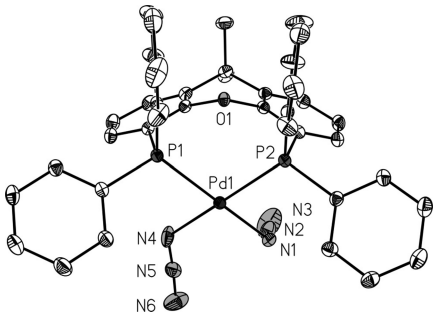


**Figure 4.** ORTEP drawing of *cis*-$[(Xantphos)Pd(N_3)_2]\cdot CHCl_3$ (***cis*-9**·$CHCl_3$) with the $CHCl_3$ molecule and all H atoms omitted and thermal ellipsoids drawn at the 50% probability level.

Xantphos at room temperature to give [(Xantphos)Pd(Ph)I] (**10**) has been reported by one of us previously.[29] We reasoned, however, that in the presence of CO, Ar−I activation with Xantphos-stabilized Pd(0) might involve mixed phosphino−carbonyl species and result in a different outcome. Surprisingly little is known about oxidative addition to Pd(0) complexes bearing both tertiary phosphine and CO ligands.[34,39]

Mixing Xantphos with $Pd_2(dba)_5$ in a 1:1 ligand to Pd ratio in benzene-$d_6$ produced two $^{31}P$ NMR-observable species, [(Xantphos)Pd(dba)] (**11**; two doublets at 11.3 and 13.5 ppm; $J_{P-P}$ = 10.6 Hz) and $[(Xantphos)_2Pd]$ (two broad multiplets at 3.5 and 6.0 ppm),[29] in a 4:1 ratio. This pattern is similar to that previously reported[17] for the 4,7-di-*tert*-butylXantphos-$Pd_2(dba)_3$ system. The structure of **11** (Figure 5) was established by an X-ray diffraction study of **11**·3THF obtained from a repeat of the reaction of Xantphos with $Pd_2(dba)_5$ in THF.

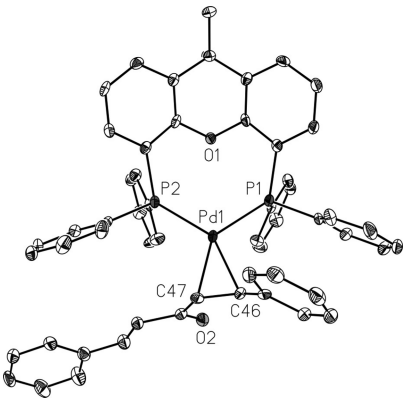


**Figure 5.** ORTEP drawing of [(Xantphos)Pd(dba)]·3THF (**11**·3THF) with the THF molecules and all H atoms omitted for clarity and thermal ellipsoids drawn at the 50% probability level.

Adding CO (1 atm) to the solution of [(Xantphos)Pd(dba)] and $[(Xantphos)_2Pd]$ generated from Xantphos and $Pd_2(dba)_5$ in benzene-$d_6$ or THF resulted in instantaneous full conversion of both complexes and the appearance of only one singlet resonance at 10.5 ppm ($C_6D_6$) in the $^{31}P$ NMR spectrum. Two strong bands at 1974 and 2014 $cm^{-1}$ in the FT-IR spectrum of the reaction solution in THF suggested[40] that the species resonating at 10.5 ppm in the $^{31}P$ NMR spectrum is a dicarbonyl complex, likely $[(Xantphos)Pd(CO)_2]$ (**12**). This structure was indeed established by a single-crystal X-ray diffraction study of **12**·hexane (Figure 6) obtained from an independent experiment (see below).

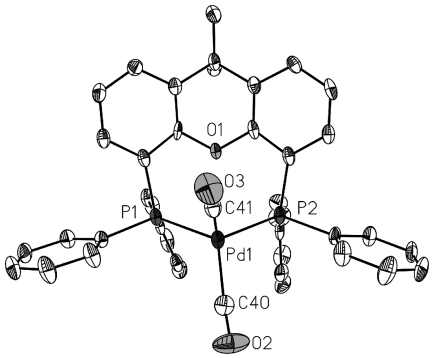


**Figure 6.** ORTEP drawing of [(Xantphos)Pd(CO)$_2$]·*n*-C$_6$H$_{14}$ (**12**·hexane) with cocrystallized hexane and all H atoms omitted and thermal ellipsoids drawn at the 50% probability level.

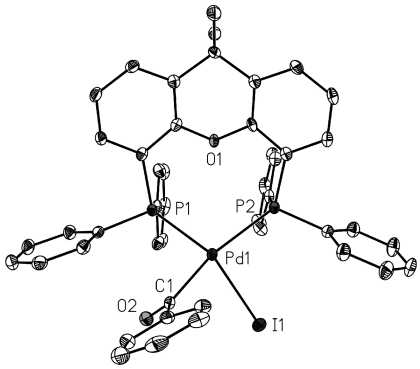


**Figure 7.** ORTEP drawing of *cis*-[(Xantphos)Pd(COPh)I]·0.5THF (***cis*-13**·0.5THF) with the THF molecule and all H atoms omitted and thermal ellipsoids drawn at the 50% probability level.[9]

We then found that bubbling argon through a solution of **12** (generated from **11** and CO) quantitatively produced **11** within 1 min. These observations clearly indicated that, although CO binds more tightly to (Xantphos)Pd(0) than dba, the formation of **12** from **11** is reversible and that the equilibrium between the two can be easily shifted to **11** under CO-deficient conditions. Both **11** and **12** were found to react with PhI. The reaction of **11** with PhI has been previously shown to produce [(Xantphos)Pd(Ph)I] (**10**; see above). In the current work, we found that **10** readily reacted with CO (1 atm) to give selectively the product of CO insertion into the Pd−Ph bond, [(Xantphos)Pd(COPh)I] (**13**), which was also formed upon addition of PhI to **12** under CO (Scheme 7). Complex **13** was isolated and fully characterized, including by single-crystal X-ray diffraction (Figure 7).[9] Like its bromo congener [(Xantphos)-Pd(COPh)Br],[15a] **13** was found to be cis in the crystal yet displayed only one $^{31}$P NMR singlet in THF, benzene, and CD$_2$Cl$_2$. Although this behavior could be attributed to **13** being exclusively trans in solution, it is likely that the complex undergoes extremely facile cis−trans isomerization that may not be frozen out on the NMR time scale. A very low barrier of only 6.1 kcal/mol has been computed for this isomerization (see below).

**Scheme 7**

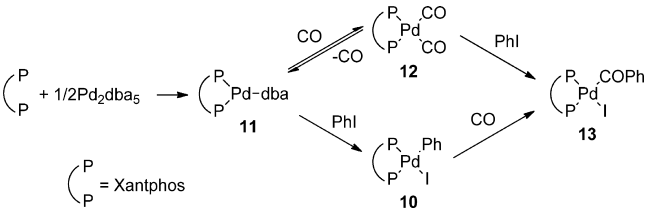


As follows from Scheme 7, there are two oxidative addition pathways leading to the key intermediate **13**. If Ar−I oxidative addition is the rate-limiting step, the catalytic process should be slower at higher concentrations of CO, favoring the formation of **12**. The latter is less electron-enriched than **11** because of the stronger $\pi$-acidity of two CO ligands in comparison with dba. Slower reaction rates under higher CO pressures have been reported[35] for Pd-catalyzed alkoxycarbonylation reactions. The literature data[41] on the solubility of CO in benzene allowed the CO to Pd ratio in our standard catalytic azidocarbonylation runs (1 atm, 25 °C) to be estimated at ca. 1:1. Under such conditions, 4-fluoroiodobenzene was azido-carbonylated at 99% conversion in 2 h. In a repeat of this run under 7 atm of CO (CO:Pd = ca. 8), only 25% conversion was reached after the same period of time, indicating that [CO] does influence the rate-limiting oxidative addition step, as shown in Scheme 7 and confirmed by the computational studies below.

Both products of the oxidative addition, **10** and **13**, were found to readily react with azide, as shown in Scheme 8. Treatment of **13** with [Bu$_4$N]$^+$N$_3^-$ in benzene[42] under CO resulted in the instantaneous clean formation of PhCON$_3$ along with [(Xantphos)Pd(CO)$_2$] (**12**). In this way, the modeled catalytic cycle was closed because PhCON$_3$ is the final product of the process and **12** can commence another turnover by Ar−I activation via the oxidative addition (Scheme 7).

Intermediate **10** that would be produced under CO-deficient conditions (Scheme 7) was also reactive toward azide (Scheme 8). The reaction of **10** with 1.1 equiv of [Bu$_4$N]$^+$N$_3^-$ in benzene produced [(Xantphos)Pd(Ph)(N$_3$)] (**14**) quantitatively. This anionic ligand exchange also readily occurred with NaN$_3$ under biphasic conditions in the absence of a phase-transfer agent. In benzene−aqueous NaN$_3$, thermodynamic equilibrium between **10** and **14** was reached within 5 min at vigorous stirring. However, only ca. 60% conversion to **14** was observed at equilibrium even in the presence of 10 equiv of NaN$_3$. To isolate **14**, the bromo analogue[43] of **10** was used, because in the presence of water the equilibrium between the Pd−X and Pd−N$_3$ (**14**) complexes is shifted more toward the latter for X = Br than for X = I[44] since bromide is more strongly hydrated than iodide. The anion exchange extraction[45] of the Br$^-$ from [(Xantphos)Pd(Ph)Br] in CH$_2$Cl$_2$ with aqueous NaN$_3$ gave **14**, which was isolated pure and fully characterized in solution by $^1$H and $^{31}$P NMR data and in the solid state by single-crystal X-ray diffraction (Figure 8).[9]

Bubbling CO through a solution of **14** in benzene-$d_6$ resulted in the instantaneous formation of PhCON$_3$ and [(Xantphos)-Pd(CO)$_2$] (**12**; Scheme 8). Repeating this reaction in toluene with subsequent addition of hexanes produced X-ray-quality crystals for the structure determination of **12** (Figure 6).

The results described above pointed clearly to two reaction pathways to PhCON$_3$ with simultaneous regeneration of Pd(0), via **13** and via **14** (Schemes 7 and 8). Both routes likely lead to [(Xantphos)Pd(COPh)(N$_3$)] (**15**) as a common intermediate that undergoes PhCO−N$_3$ reductive elimination. The competition between these two reaction channels is expected to be strongly dependent on the concentrations of CO and N$_3^-$, the nature of the medium, and other factors that control anionic

**Scheme 8**

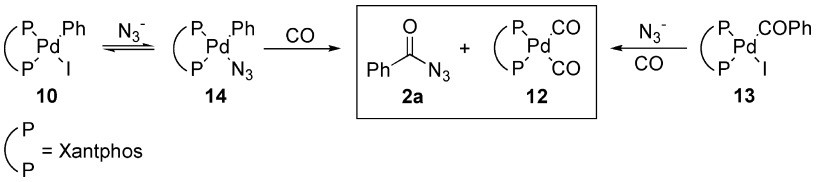


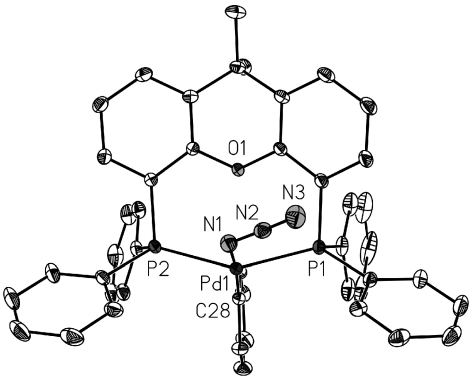


**Figure 8.** ORTEP drawing of *trans*-[(Xantphos)Pd(Ph)($N_3$)] (***trans*-14**) with all H atoms omitted and thermal ellipsoids drawn at the 50% probability level.[9]

ligand exchange and migratory insertion processes as well as mass transfer in the triphasic liquid–liquid–gas system. Two extreme cases could be considered. If the catalytic reaction is performed in the presence of CO in excess ([Pd] ≪ [CO]), the pathway involving **13** is expected to dominate because the facile migratory insertion of CO into the Pd–C bond of **10** is a homogeneous process rapidly occurring in the organic phase, whereas the alternative route, via **14**, requires slower anionic ligand exchange at the liquid–liquid interface of the biphasic system. The prevailing catalytic cycle would then involve the sequence **12** → **10** → **13** → **15** → **12** (loop A in Scheme 9). It remains unknown if the oxidative addition of ArI to **12** occurs via predissociation of both carbonyl ligands from the Pd center. If it does, then **10** is likely involved in the cycle, albeit as a short-lived intermediate that is quickly transformed to **13** via facile CO insertion. However, if at least one CO ligand remains on Pd during the Ar–I oxidative addition, the formation of **10** might be skipped, with **12** going directly to **13**, i.e., **12** → **13** → **15** → **12** (Scheme 9, loop B). Under CO-deficient conditions ([Pd] > [CO]), two other catalytic pathways are possible: **11** → **10** → **13** → **15** → **11** (loop C) and **11** → **10** → **14** → **15** → **11** (loop D). The competition between loops C and D would obviously depend on relative rates of the transformation of **10**

**Scheme 9**

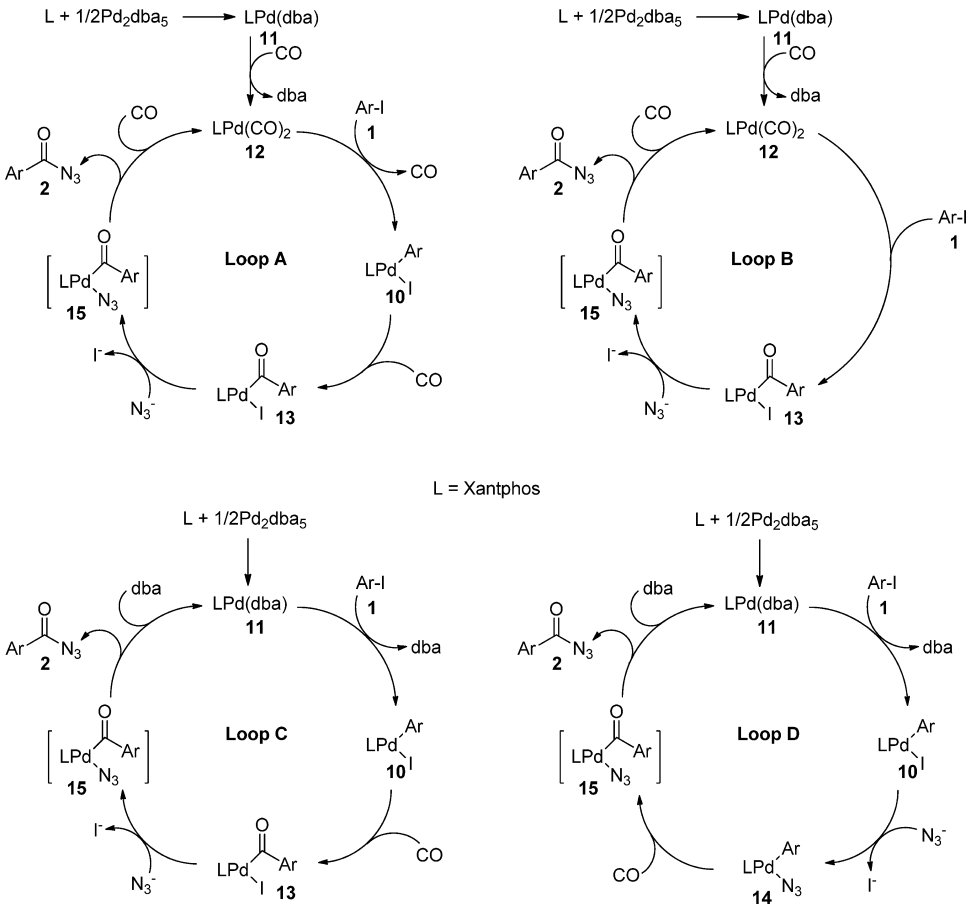

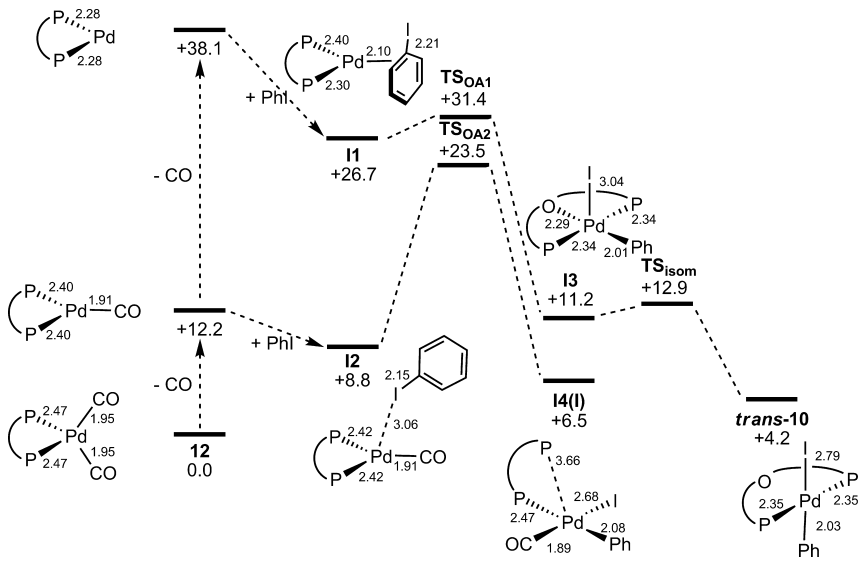


**Figure 9.** Alternative computed reaction profiles for PhI activation at [(Xantphos)Pd(CO)$_2$] (**12**). Relative free energies in water are given in kcal/mol.

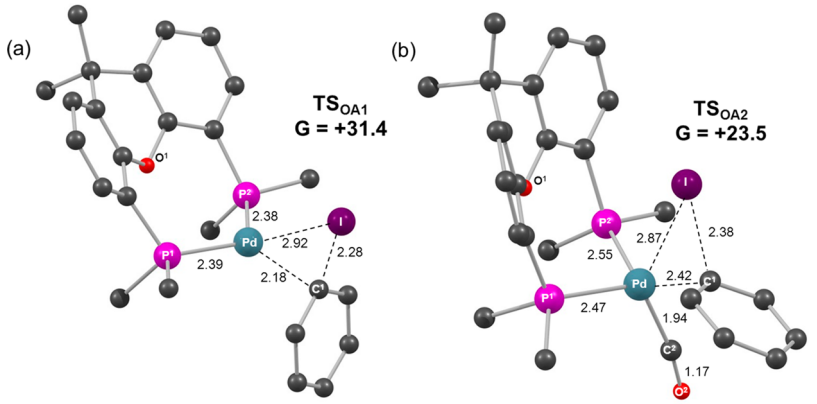


**Figure 10.** Computed transition state geometries for Ph−I activation at (a) [(Xantphos)Pd] and (b) [(Xantphos)Pd(CO)]. Relative free energies in water are given in kcal/mol as well as selected distances in Å. Xantphos Ph groups are truncated at the ipso carbon and H atoms are omitted for clarity.

to **13** (CO insertion) and to **14** ($I^-/N_3^-$ exchange), as well as of carbonylation of **14** to **15**. As described above, the possibility for all four pathways A−D (Scheme 9) has been demonstrated by stoichiometric experiments. Regardless of which of the reaction channels wins the competition, the process invariably leads to the desired aroyl azide product. Importantly, unlike [$(R_3P)_2Pd(Ph)(N_3)$][7] (R = Me, Et; see above), **14** does *not* form a Pd-NCO species via $N_2$ loss upon treatment with CO.

In our experimental mechanistic studies, we have succeeded in the isolation and full characterization of all intermediates involved in the azidocarbonylation process (Schemes 7−9; Ar = Ph), except for [(Xantphos)Pd(COPh)($N_3$)] (**15**). As **15** is too unstable for isolation and/or detection, quickly undergoing reductive elimination of $PhCON_3$, we studied the various mechanistic routes to this species and the subsequent product-forming C−N bond coupling event by computational means.

## ■ COMPUTATIONAL STUDIES

Density functional theory (DFT) calculations have been employed to assess the different mechanistic possibilities outlined in Scheme 9. Throughout we report free energies corrected for water solvent using a BP86-D3(BS2)//BP86-(BS1) protocol, i.e. based on free energies derived from gas-phase optimizations computed with a smaller basis set (BS1), and adding to this corrections for solvation (water, PCM approach computed with BS1), dispersion, and basis effects, the last via recomputation of the SCF energy with a larger basis set (BS2) (see Computational Details).

We first considered the different species that may be involved in the initial Ph−I oxidative addition step under conditions of excess CO (i.e., loop A vs loop B; Scheme 9). The most stable Pd(0) precursor under these circumstances is [(Xantphos)Pd-(CO)$_2$] (**12**; $G$ = 0.0 kcal/mol), and successive CO dissociations from this species lead to trigonal-planar [(Xantphos)Pd(CO)] ($G$ = +12.2 kcal/mol) and [(Xantphos)-Pd] ($G$ = +38.1 kcal/mol; see Figure 9). PhI can add to the latter to give an $\eta^2$-adduct bound through the $C_{ipso}$−$C_{ortho}$ bond (**I1**; G = +26.7 kcal/mol) which is the direct precursor to C−I cleavage. This proceeds with a small additional barrier of 4.7 kcal/mol through a pseudotetrahedral transition state (**TS$_{OA1}$**; see Figure 10(a)) which leads initially to **I3** (G = +11.2 kcal/mol), an isomer of **10** featuring a square-pyramidal geometry with a weakly bound axial iodide and a $\kappa^3$-P,O,P Xantphos ligand.[46] Elongation of the Pd−O bond leads to ***trans*-10** (G =

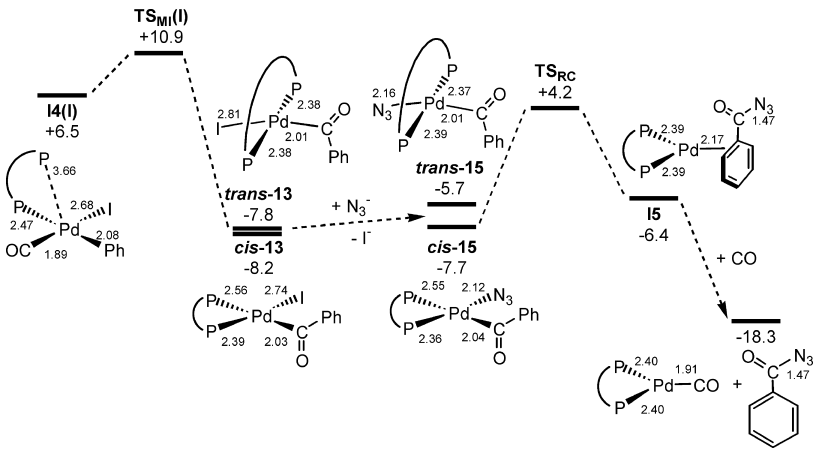


**Figure 11.** Computed reaction profiles for the formation of [(Xantphos)Pd(CO)] and $PhCON_3$ from **I4(I)** + $N_3^-$. Relative free energies in water are given in kcal/mol.

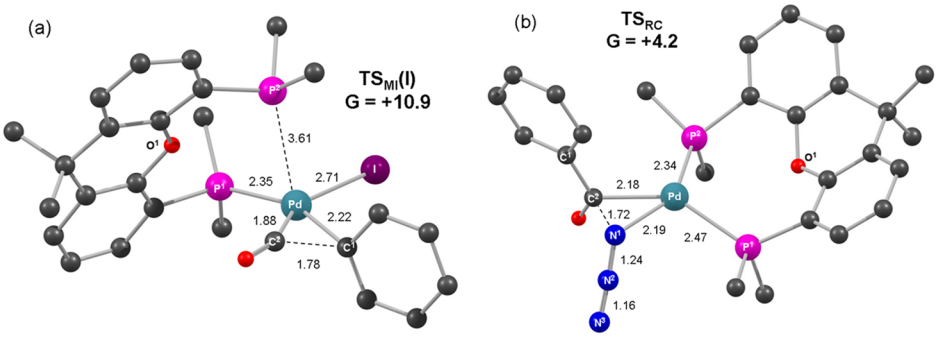


**Figure 12.** Computed transition states for (a) CO migratory insertion in [(Xantphos)Pd(CO)(I)(Ph)] (**I4(I)**) and (b) C−N reductive coupling in *cis*-[(Xantphos)Pd(COPh)($N_3$)] (***cis*-15**). Relative free energies in water are given in kcal/mol and selected distances in Å. Xantphos Ph groups are truncated at the ipso carbon, and hydrogen atoms are omitted for clarity.

+4.2 kcal/mol) with a minimal barrier of 1.7 kcal/mol via $\mathbf{TS_{isom}}$. Alternatively, Ph−I cleavage may occur at [(Xantphos)-Pd(CO)]. In this case no $\eta^2$-adduct could be located, possibly due to increased steric encumbrance around the Pd center; instead, the most stable precursor located is a noncovalently bound adduct in which PhI lies above the metal coordination plane with the iodine directed toward the Pd center (**I2**; Pd···I = 3.06 Å; $G$ = +8.8 kcal/mol). From here Ph−I bond cleavage occurs via $\mathbf{TS_{OA2}}$ ($G$ = +23.5 kcal/mol) which displays a distorted trigonal-bipyramidal geometry with CO and I in the axial sites (see Figure 10(b)). $\mathbf{TS_{OA2}}$ also features significant elongation of the Pd−P2 distance (by ca. 0.14 Å cf. **I2**), and IRC calculations show that this bond breaks completely in forming intermediate **I4(I)** (Pd···P2 = 3.66 Å; $G$ = +6.5 kcal/mol). **I4(I)** displays a square-planar coordination geometry around Pd with CO again trans to I, this being favored (as in $\mathbf{TS_{OA2}}$) due to the trans arrangement of $\pi$-acceptor and $\pi$-donor ligands. Figure 9 shows that Ph−I bond activation is most accessible via [(Xantphos)Pd(CO)] and proceeds with an overall barrier of 23.5 kcal/mol to form [(Xantphos)Pd(CO)-(I)(Ph)] directly, i.e., suggesting that loop B will be in operation (Scheme 9).

We have also considered Ph−I activation under low CO concentrations. Under these conditions the likely Pd(0) precursor is [(Xantphos)Pd(dba)] (**11**), which is computed to lie 10.0 kcal/mol above [(Xantphos)Pd($CO)_2$]. The estimated barrier (via $\mathbf{TS_{OA1}}$) would therefore be 21.4 kcal/mol, assuming facile displacement of dba by PhI, and this is consistent with more facile aryl halide activation in the absence of CO noted above.

The computed reaction profile for the remainder of the catalytic cycle along loop B is shown in Figure 11. CO migratory insertion in **I4(I)** proceeds via $\mathbf{TS_{MI}(I)}$ with a barrier of 4.4 kcal/mol and forms ***trans*-13** at −7.8 kcal/mol,[47] which is computed to be 0.4 kcal/mol less stable than ***cis*-13** in solution. Formation of ***cis*-15** may proceed via trans−cis isomerization in **13** and $I^-/N_3^-$ exchange or via $I^-/N_3^-$ exchange in ***trans*-13** followed by trans−cis isomerization in **15**. Both possibilities appear to be readily accessible, for example, trans−cis isomerization in **13** has a barrier of only 6.1 kcal/mol, while both $I^-/N_3^-$ exchange processes are computed to lie close to equilibrium.[48] Once ***cis*-15** is formed, C−N bond formation proceeds via $\mathbf{TS_{RC}}$ with a barrier of 11.9 kcal/mol, readily accessible at room temperature and so consistent with **15** being unobserved experimentally.[49] This gives **I5**, the most stable form of which has $PhCON_3$ bound as an $\eta^2$-arene fashion through a $C_{ipso}$−$C_{ortho}$ bond ($G$ = −6.4 kcal/mol). The $PhCON_3$ product can then be displaced from **I5** by CO to regenerate [Pd(Xantphos)(CO)]. Each of these steps is readily accessible and the calculations suggest that after rate-limiting oxidative addition the formation of products and regeneration of the catalyst **12** will be rapid and strongly exergonic ($\Delta G$ = −30.4 kcal/mol). Computed geometries for $\mathbf{TS_{MI}(I)}$ and $\mathbf{TS_{RC}}$ are both shown in Figure 12, and all other geometries are given in the Supporting Information.

Further calculations probed the effect of $I^-/N_3^-$ exchange on the migratory insertion process. $I^-/N_3^-$ substitution in **I4(I)** gives **I4($N_3$)** ($G$ = +6.0 kcal/mol), in which azide is now trans to CO. Thus, $I^-/N_3^-$ exchange is again close to equilibrium ($\Delta G$ = −0.5 kcal/mol), although the subsequent migratory insertion transition state is now less accessible than for the iodide analogue (**$TS_{MI}$($N_3$)**: $G$ = +15.4 kcal/mol cf. **$TS_{MI}$(I)** at +10.9 kcal/mol). Both processes are more accessible than the preceding (overall rate-limiting) Ph−I oxidative addition, and so a proportion of the catalysis could therefore proceed through **I4($N_3$)** leading to the direct formation of ***trans*-15**.

## ■ DISCUSSION

**Selectivity, Efficiency, Scope, and Limitations of the Reaction.** The azidocarbonylation reaction represents a novel, methodologically distinct approach to aroyl azides. While all previously developed methods to synthesize $ArCON_3$ employ starting materials that already include the carbonyl moiety,[3] our reaction constructs the desired product of ArI, CO, and $N_3^-$ at the metal center of a Pd catalyst. The uniquely remarkable catalytic activity of the Pd−Xantphos system identified here allows numerous problems to be obviated that otherwise would prevent the azidocarbonylation from occurring. As discussed in the Introduction, those include the thermal decomposition of the product (Curtius rearrangement), catalyst deactivation from the exceedingly facile Staudinger reaction of the aroyl azide produced with the stabilizing tertiary phosphine on the metal, and transformation of the $N_3$ ligand on Pd to NCO with concomitant loss of $N_2$ (Schemes 1−3).

Efficiently catalyzed by the Pd-Xantphos system, the azidocarbonylation reaction has a broad scope and can be used with a wide variety of meta- and para-substituted aryl iodides. Functional groups such as alkyl, alkoxy, acyl, alkoxycarbonyl, nitro, cyano, and even formyl are easily tolerated. Although the reaction readily occurs at room temperature and atmospheric pressure, it is inapplicable to the synthesis of ortho-substituted aroyl azides that are intrinsically less stable toward the Curtius rearrangement. The isocyanates thus formed in the reaction are then involved in subsequent transformations in situ, leading to other products, including ureas (Scheme 5).

The catalyst deactivation study identified [(Xantphos)$PdI_2$] (**7**) as the main product of catalyst poisoning. Since fortuitously no structural changes to the Xantphos ligand are involved in the deactivation process, the nonorganometallic Pd(II) complex **7** can be reduced in situ to Pd(0), thereby regaining the catalytic activity. The identification of readily available and cheap PMHS as the particularly efficient reducing agent for this purpose has led to the development of the markedly efficient process employing only 0.2 mol % of easily accessible, air-stable [(Xantphos)$PdCl_2$] (**8**) as added catalyst. Cross-coupling reactions of haloarenes employing such a low Pd catalyst loading are rare. Considering the above-explained vulnerability of the reaction, it is truly remarkable that nearly quantitative conversions can be achieved with such small quantities of the catalyst. Furthermore, the reaction exhibits >85% selectivity if run under optimized conditions. The low catalyst loading in combination with the high conversion and selectivity allow the straightforward and safe preparation of pure aroyl azides in ca. 80−90% isolated yield on a 1−2 g scale. Nonetheless, if an aroyl azide is desired for a further transformation, such as to the corresponding isocyanate, benzamide, iminophosphorane, etc., those reactions may be performed in situ, without isolation of the originally produced $ArCON_3$ (Scheme 6).

The biggest drawback of the Pd-catalyzed azidocarbonylation is its inapplicability to aryl bromides. Being less reactive than aryl iodides, bromoarenes can be activated via oxidative addition to Xantphos-stabilized Pd(0) only at elevated temperatures that aroyl azides do not survive. Furthermore, diminished stability constants of various Pd(Xantphos) units involved in the catalysis at higher temperatures facilitate the Staudinger reaction leading to catalyst deactivation, as described above. It is particularly important that Ar−X activation with phosphine-stabilized Pd(0) takes place with a higher activation barrier in the presence than in the absence of CO. Our studies shed new light on this poorly studied and understood key mechanistic feature (see below).

**Reaction Mechanism.** The azidocarbonylation reaction occurs under triphasic liquid−liquid−gas conditions. Aside from mass transfer that clearly depends on such parameters as agitation rate and pressure, the rate-determining step of the catalytic process is Ar−I activation with Pd(0). Since the pioneering work of Fitton and co-workers,[50] oxidative addition of haloarenes to tertiary phosphine complexes of zerovalent palladium has been studied in considerable detail.[51] Migratory insertion of CO into a variety of complexes of the type [($R_3P$)M(Ar)X] (M = Pt, Pd, Ni) has been thoroughly studied in the classic paper by Garrou and Heck.[6] Strikingly, however, very little mechanistic information has been reported on oxidative addition of aryl halides to tertiary phosphine-stabilized Pd(0) complexes in the presence of CO, i.e., under the catalytic conditions of the Heck carbonylation that has been known and widely used for nearly 40 years.[1]

The experimental and computational results obtained in the current work allow us to analyze two extreme cases: (1) the catalytic reaction is carried out with CO in excess ([Pd] < [CO]; loops A and B in Scheme 9) and (2) the process occurs under CO-deficient conditions ([Pd] > [CO]; loops C and D in Scheme 9). The experimentally observed slower reaction rate at higher concentrations of CO (see above) is in accord with the computational results. The prohibitively high barrier (38.1 kcal/mol) to the loss of both carbonyl ligands from the (Xantphos)$Pd^0$ moiety (Figure 9) rules out Ar−I oxidative addition to the carbonyl-free Pd(0) in the presence of CO in excess. Dissociation of only one CO from [(Xantphos)Pd-$(CO)_2$], however, occurs with a much lower free energy cost of only 12.2 kcal/mol, suggesting that [(Xantphos)Pd(CO)] is accessible. (In the presence of larger quantities of CO, the equilibrium between the two is obviously shifted to the unreactive dicarbonyl complex.) Furthermore, it has been demonstrated by the calculations that the monocarbonyl [(Xantphos)Pd(CO)] can activate the Ph−I bond with an overall barrier of 23.5 kcal/mol. This is reasonably consistent with the estimated value $\Delta G^{\ddagger} \approx 21.5 \pm 0.5$ kcal/mol at 296 K from the experimental data for oxidative addition of 4-$FC_6H_4I$ to [(Xantphos)Pd$(CO)_2$] (**12**; see the Supporting Information). However, [(Xantphos)Pd(Ar)(I)] is not on the reaction coordinate in this case and the process is mediated by [(Xantphos)Pd(CO)(Ar)(I)], leading to [(Xantphos)Pd-(COAr)I], as shown in Figure 11 for Ar = Ph. Therefore, in the presence of CO in excess, the reaction is governed by loop B, not A (Scheme 9).

We define CO-deficient conditions as [Pd] ≈ [CO] or [Pd] > [CO] and the CO diffusion rate is slower than that of the catalytic reaction. Under such conditions, loops C and D

(Scheme 9) are expected to be operational, since the Pd(0) produced in the product-forming step would undergo fast Ar−I oxidative addition before the CO consumed in the catalytic cycle is replenished from the gas phase. With [(Xantphos)Pd(dba)] (**11**) as the resting state of the Pd(0) form of the active catalyst, the computed barrier is 21.4 kcal/mol (see above). The resultant stable and isolable[29] intermediate [(Xantphos)Pd(Ph)(I)] (**10**) can then either undergo carbonylation to [(Xantphos)Pd(COPh)I] (**13**) when CO becomes available (loop C) or react with azide to form [(Xantphos)Pd(Ph)($N_3$)], (**14**; loop D). Mass transfer is involved in both processes since the Pd catalyst is located in the organic phase, the azide source ($NaN_3$) is in the immiscible aqueous layer, and CO is in the headspace. Although under anhydrous conditions the experimentally observed equilibrium between **10** and **14** is shifted entirely to the latter,[52] in benzene−aqueous $NaN_3$ both are present in comparable quantities (see above). However, **10** and **14** exhibit different reactivities toward CO. The computed data (in water) suggest that migratory insertion of CO into the Pd−C bond of **10** is $>10^3$ times faster than that of **14**. This indicates that if CO diffusion into the organic phase is slower than the iodide/azide ligand exchange, of the two loops C and D it is the former that will be by far the largest contributor to the overall catalytic transformation. The influence of the anionic ligand X on both kinetics and thermodynamics of the reactions of [$(R_3P)_2$Pd(Ar)X] with CO has long been recognized.[6] For instance, [$(Ph_3P)_2$Pd(Ar)X] species undergo full conversion to the corresponding [$(Ph_3P)_2$Pd(COAr)X] more rapidly for X = I than for X = Br (Ar = 4-$NO_2C_6H_4$ or 4-$NCC_6H_4$). However, CO insertion into the Pd−Ph bond of [$(R_3P)_2$Pd(Ph)Cl] is reversible for both R = Ph[6] and Cy.[53]

As seen from the above, three different catalytic cycles (loops B−D in Scheme 9) can govern the azidocarbonylation reaction. With CO in excess in the organic phase, loop B is operational. Under CO-deficient conditions, loops C and (to a much smaller extent) D operate the process. It is quite possible that under the conditions conventionally used in the current work, i.e. [Pd] ≈ [CO] in the organic phase at 1 atm (see above), the reaction occurs largely via the C channel at the beginning when the concentration of the iodoarene substrate is high and the rate-limiting oxidative addition is faster than CO mass transfer. The formation of less reactive Pd(0) carbonyls is skipped in this way and, as a result, it is the more reactive CO-free Pd(0) that effects the Ar−I oxidative addition. As [ArI] drops during the reaction, the rate of its oxidative addition first becomes comparable with, and eventually slower than, the CO diffusion rate which is constant. In other words, the mechanism that operates at the beginning of the reaction (loop C) is gradually replaced with the other, higher barrier channel (loop B). Poorly efficient azide/iodide ligand exchange in the organic solvent−water biphasic system (e.g., slow agitation) would result in accumulation of stable [(Xantphos)Pd(COPh)I] (**13**) and consequently higher concentrations of CO, thus favoring the more energy demanding channel (loop B). The diminished reactivity of aryl bromides prohibits the intrinsically faster catalytic cycles C and D from operation because Ar−Br oxidative addition to Pd(0) is considerably slower than CO mass transfer under the standard reaction conditions. The only mechanistic option left for aryl bromides is loop B that involves the less reactive form of Pd(0), [(Xantphos)Pd$(CO)_2$] (**12**).

**Potential Applications in $^{11}$C Radiolabeling.** $^{11}$C positron emission tomography (PET) is a powerful diagnostic tool that currently employs $^{11}CO_2$, $^{11}CH_3I$, and $^{11}$CO precursors for the preparation of radiotracers.[54] The short lifetime of the $^{11}$C isotope ($t_{1/2}$ = 20.4 min) dictates the need for highly efficient and selective organic transformations that produce the desired $^{11}$C-containing product within ca. 10 min. Pd-catalyzed carbonylation reactions have been used to produce $^{11}$C-labeled aldehydes, ketones, carboxylic acids, and their derivatives.[54,55] Very recently, an efficient protocol with a Pd-Xantphos catalyst was developed.[55d]

Under optimized conditions, the azidocarbonylation reaction occurs on the time scale that might be suitable for $^{11}$C PET. For instance, 85% conversion of 4-fluoroiodobenzene was achieved in 10 min, using the standard protocol. In another experiment using 1 equiv of CO, 4-fluorobenzoyl azide was cleanly produced in 66% yield in 5 min (see the Supporting Information). It is believed that the azidocarbonylation reaction may find applications in $^{11}$C PET, considering (i) the appropriate time scale, (ii) the fact that aroyl azides are highly reactive and versatile reagents in synthesis,[3] and (iii) the demonstrated possibility to use the Ar$CON_3$ product for further transformations without isolation (Scheme 6).

**Why Xantphos?** Of numerous tertiary phosphines screened in the current work, Xantphos is the only efficient ligand for the Pd-catalyzed azidocarbonylation reaction. The well-established remarkable catalytic activity of Xantphos-stabilized transition-metal complexes[14] is often attributed to its wide bite angle. It has been recently demonstrated,[30] however, that factors other than that may be involved. To understand the origin of the uniquely excellent performance of the Xantphos-Pd catalyst in the azidocarbonylation reaction, a separate mechanistic study is needed, similar to that performed in the current work but with analogous Pd complexes bearing ligands other than Xantphos.

## ■ CONCLUSIONS

We have discovered the first aromatic azidocarbonylation reaction, the formation of aroyl azides from aryl iodides, CO, and $NaN_3$ in the presence of a Pd catalyst. This transformation is vastly more challenging than other Heck-type Pd-catalyzed carbonylation reactions because (i) the product, Ar$CON_3$, is thermally unstable (Curtius rearrangement) under conventional ArX carbonylation conditions, (ii) the Pd catalyst may be easily and irreversibly deactivated by the exceedingly facile Staudinger reaction of the aroyl azide product with the stabilizing tertiary phosphine ligand, and (iii) the azido ligand on Pd may react with CO to give isocyanate with concomitant loss of $N_2$.[7] Remarkably, all these problems are obviated by the use of the unique Pd-Xantphos catalytic system that effects the transformation in an organic solvent−$H_2O$ biphasic system at room temperature and 1 atm of CO. The catalytic process exhibits high efficiency and functional group tolerance.

A catalyst poisoning study has shown that the deactivation process does not involve structural changes of the stabilizing ligand but rather leads to the catalytically inactive non-organometallic complex [(Xantphos)Pd$I_2$]. This has allowed us to find a way to revitalize the poisoned catalyst by performing the reaction in the presence of cheap and readily available PMHS that reduces the inactive Pd(II) to catalytically active Pd(0). As a result, the catalyst loading has been lowered from 2% to 0.2% without any losses in selectivity at nearly 100% conversion. The synthetic value of the process with this uncommonly low catalyst loading has been demonstrated by the successful synthesis of a series of aroyl azides as spectroscopically and analytically pure compounds in ca. 80−90% isolated yield on a gram scale. Alternatively, the products

may not be isolated but rather used in situ for further transformations such as the synthesis of isocyanates, ureas, benzamides, iminophosphoranes, etc.

Like any other process, the azidocarbonylation reaction has limitations. First, it is inapplicable to aryl bromides that are activated by Pd(0) at temperatures that prompt the rearrangement of the aroyl azide product and its reaction with the stabilizing phosphine ligand, which leads to catalyst deactivation. Second, ortho-substituted iodoarenes, when azidocarbonylated, give rise to the corresponding $ArCON_3$ that are innately less stable toward the Curtius rearrangement. In certain cases, the reaction of ortho-substituted substrates can produce the corresponding symmetric ureas in good yield.

A detailed mechanistic study of the azidocarbonylation reaction by experimental and computational means has shown that two main reaction pathways can operate in the process. Oxidative addition of the Ar−I bond to Pd(0) is the rate-determining step of both routes. In the presence of excess CO, the Ar−I bond is activated by the less electron-rich Pd center of a mixed carbonyl phosphine complex. Under CO-deficient conditions, a lower energy barrier pathway is followed, involving Ar−I oxidative addition to a more reactive carbonyl -free Xantphos-stabilized Pd(0) species. Mass transfer in the triphasic liquid−liquid−gas system used in the current work plays an important role in the competition between these two mechanistic routes, uniformly leading to a common aroyl azido intermediate that undergoes $ArCO-N_3$ reductive elimination.

It is hoped that the novel azidocarbonylation reaction will find applications in the synthesis of some otherwise poorly accessible aroyl azides and that the previously unavailable mechanistic information will be of help in the design and optimization of other Pd-catalyzed carbonylation reactions of aromatic electrophiles.

## ■ EXPERIMENTAL SECTION

*Caution! Care should be exercised when handling azide derivatives that may be potentially explosive. Exposing phosphine-free palladium compounds to a source of azide must be avoided in order to eliminate the risk of generating highly explosive, shock-sensitive materials.*[38] *Aroyl azides, pure or in solution, should not be exposed to temperatures exceeding 60 °C to avoid decomposition via the Curtius rearrangement.*

All chemicals were purchased from Aldrich, Alfa Aesar, TCI, Deutero, and Pressure Chemical. Benzene, toluene, THF, dichloromethane, hexanes, and other solvents were used as received, unless otherwise noted. Anhydrous, oxygen-free benzene, benzene-$d_6$, toluene, xylenes, THF, and hexanes for mechanistic studies were obtained by distillation from $Na/OCPh_2$. $CD_2Cl_2$ and $CDCl_3$ were vacuum-transferred from $CaH_2$. All solvents for experiments under an inert atmosphere were stored over freshly activated 4 Å molecular sieves in a glovebox. Column chromatography was performed on 60A silica gel (40−63 μm). The complexes $Pd_2(dba)_3$,[13] [(Xantphos)Pd(Ph)I] (**10**),[29] $[(Ph_3P)_2Pd(Ph)Br]$,[56] $[(Xantphos)PdCl_2]\cdot CH_2Cl_2$ (**8**),[57] [(Xantphos)Pd(COPh)I] (**13**),[9] and $[(Xantphos)Pd(Ph)N_3]$ (**14**)[9] were prepared by the literature procedures. $^1H$, $^{19}F$, and $^{31}P$ NMR spectra were recorded on Bruker Avance 400 Ultrashield and Bruker Avance 500 Ultrashield NMR spectrometers. Single-crystal X-ray diffraction studies were performed on a Bruker-Nonius diffractometer and a Bruker Apex DUO Kappa 4-axis diffractometer equipped with APEX 2 4K CCD area detectors. An Agilent Technologies 7890A-5975C instrument was used for GC-MS analysis. FT-IR measurements in solution were performed with a Thermo Nicolet FT-IR 5700 Nexus spectrometer equipped with a DLaTGS detector and a KBr beam splitter at 4 $cm^{-1}$ resolution. A Bruker Optics FTIR Alpha spectrometer with a DTGS detector and a KBr beam splitter at 4 $cm^{-1}$ resolution was used for FT-IR measurements of solid samples. Elemental analyses were performed by the Microanalysis Center at the Complutense University of Madrid. Detailed procedures for the azidocarbonylation in the absence of reducing agents (2% Pd; Table 1) can be found in the preliminary communication.[9]

**General Procedure for Azidocarbonylation of Aryl Iodides in the Presence of PMHS (0.2% Pd).** A 25 mL round-bottom flask equipped with a gas inlet and a Teflon-coated magnetic stir bar was charged, in air, with an iodoarene (10.0 mmol), $NaN_3$ (0.78 g; 12 mmol), $[(Xantphos)PdCl_2]\cdot CH_2Cl_2$ (**8**; 17 mg; 0.2 mol %), $K_2CO_3$ (28 mg; 2 mol %), and water (2 mL). After two freeze−pump−thaw cycles, the flask was back-filled with CO and connected to a CO balloon via a 1.2 mm diameter stainless steel syringe needle. With vigorous stirring, a solution of PMHS (150 mg; 25 mol %) in oxygen-free THF was syringed in and the mixture was agitated at room temperature. After GC-MS analysis of the organic phase indicated 95−100% conversion of the iodoarene, the product was isolated and purified in air. The reaction mixture was diluted with ether (10 mL) and transferred to a separatory funnel. The reaction flask was rinsed with ether (2 × 10 mL) and water (10 mL), and the washings were added to the separatory funnel. After shaking, the organic phase was separated and the aqueous phase was washed with $Et_2O$ (2 × 20 mL). The combined extract and the washings were dried over $MgSO_4$, filtered, and rotary-evaporated at room temperature. Silica gel column chromatography of the residue gave the pure product (see below and the Supporting Information for specifics).

*Benzoyl Azide (**2a**).* Azidocarbonylation of iodobenzene (2.04 g) by the general procedure using a solution of PMHS in THF (0.5 mL) gave >99% conversion after 20 h. Pentane−ether (9:1 v/v) was used for isolation by column chromatography. After solvent removal and drying on a rotary evaporator (100 mbar for 1 h, then 80 mbar for 0.5 h), **2a** was obtained as a colorless oil that crystallized on standing at +8 °C. The yield was 1.29 g (88%). $^1H$ NMR (500 MHz, $CDCl_3$): δ 7.46 (m, 2H), 7.62 (m, 1H), 8.03 (m, 2H).[9]

*4-Methylbenzoyl Azide (**2b**).* Azidocarbonylation of 4-iodotoluene (2.18 g) by the general procedure using a solution of PMHS in THF (0.5 mL) gave >99% conversion after 16 h. Hexane−ether (9:1 v/v) was used for isolation by column chromatography. After solvent removal and drying on a rotary evaporator, **2b** was obtained as a colorless oil that crystallized on standing at +8 °C. The yield was 1.33 g (83%). $^1H$ NMR (400 MHz, $CDCl_3$): δ 2.42 (s, 3H, Me), 7.25 (m, 2H), 7.92 (m, 2H).[9]

*4-Methoxybenzoyl Azide (**2d**).* Azidocarbonylation of 4-iodoanisole (2.34 g) by the general procedure using a solution of PMHS in THF (2.0 mL) gave 95% conversion after 44 h. Hexane−ether (14:1 v/v) was used for isolation by column chromatography. After solvent removal and drying on a rotary evaporator, **2d** was obtained as a white crystalline solid. The yield was 1.38 g (78%). $^1H$ NMR (400 MHz, $CDCl_3$): δ 3.87 (s, 3H, OMe), 6.93 (m, 2H), 7.99 (m, 2H).[9]

*4-Nitrobenzoyl Azide (**2e**).* Azidocarbonylation of 4-nitroiodobenzene (2.49 g) by the general procedure using a solution of PMHS in THF (3.0 mL) gave >99% conversion after 19 h. Hexane−ether (2:1 v/v) was used for isolation by column chromatography. After solvent removal and drying on a rotary evaporator, **2e** was obtained as yellowish crystals. The yield was 1.66 g (86%). $^1H$ NMR (500 MHz, $CDCl_3$): δ 8.21 (m, 2H), 8.31 (m, 2H).[9]

*4-Acetylbenzoyl Azide (**2f**).* Azidocarbonylation of 4-iodoacetophenone (2.46 g) by the general procedure using a solution of PMHS in THF (3.0 mL) gave >99% conversion after 16 h. Hexane−ether (2:1 v/v) was used for isolation by column chromatography. After solvent removal and drying on a rotary evaporator, **2f** was obtained as white crystals. The yield was 1.65 g (87%). $^1H$ NMR (400 MHz, $CDCl_3$): δ 2.65 (s, 3H, Me), 8.02 (m, 2H), 8.12 (m, 2H).[9]

*Ethyl 4-(Azidocarbonyl)benzoate (**2g**).* Azidocarbonylation of ethyl 4-iodobenzoate (2.76 g) by the general procedure using a solution of PMHS in THF (0.5 mL) gave 99% conversion after 16 h. Hexane−ether (14:1 v/v) was used for isolation by column chromatography. After solvent removal and drying on a rotary evaporator, **2g** was obtained as white crystals. The yield was 1.89 g (86%). $^1H$ NMR (400 MHz, $CDCl_3$): δ 1.41 (t, $J$ = 7.1 Hz, 3H, $CH_3$), 4.41 (q, $J$ = 7.1 Hz, 2H, $CH_2$), 8.10 (m, 4H).[9]

*4-Fluorobenzoyl Azide (2j).* Azidocarbonylation of 1-fluoro-4-iodobenzene (2.22 g) by the general procedure using a solution of PMHS in THF (0.5 mL) gave >99% conversion after 20 h. Pentane−ether (9:1 v/v) was used for isolation by column chromatography. After solvent removal and drying (100 mbar for 1 h) on a rotary evaporator, **2j** was obtained as a colorless oil. The yield was 1.42 g (86%). $^1$H NMR (500 MHz, $CDCl_3$): $\delta$ 7.12 (m, 2H), 8.05 (m, 2H). $^{19}$F{$^1$H} NMR (377 MHz, $CDCl_3$): $\delta$ −102.7 (s).[9]

*4-Chlorobenzoyl Azide (2k).* Azidocarbonylation of 1-chloro-4-iodobenzene (2.39 g) by the general procedure using a solution of PMHS in THF (0.5 mL) gave >99% conversion after 20 h. Hexane−ether (9:1 v/v) was used for isolation by column chromatography. After solvent removal and drying on a rotary evaporator, **2k** was obtained as a white crystalline solid. The yield was 1.60 g (88%). $^1$H NMR (500 MHz, $CDCl_3$): $\delta$ 7.44 (m, 2H), 7.97 (m, 2H).[9]

*3-Methoxybenzoyl Azide (2o).* Azidocarbonylation of 3-iodoanisole (2.34 g) by the general procedure using a solution of PMHS in THF (0.5 mL) gave >99% conversion after 19 h. Hexane−ether (9:1 v/v) was used for isolation by column chromatography. After solvent removal and drying on a rotary evaporator, **2o** was obtained as a colorless oil. The yield was 1.57 g (89%). $^1$H NMR (500 MHz, $CDCl_3$): $\delta$ 3.86 (s, 3H, OMe), 7.16 (ddd, $J$ = 8.3, 2.6, and 1.0 Hz, 1H), 7.36 (t, $J$ = 8.0 Hz, 1H), 7.54 (dd, $J$ = 2.6 and 1.6 Hz, 1H), 7.62 (ddd, $J$ = 7.7, 1.6, and 1.0 Hz, 1H).[9]

*2-Thiophenecarbonyl Azide (2q).* Azidocarbonylation of 2-iodothiophene (2.10 g) by the general procedure using a solution of PMHS in THF (0.5 mL) gave >99% conversion after 17 h. Pentane−ether (9:1 v/v) was used for isolation by column chromatography. After solvent removal and drying (100 mbar for 1 h) on a rotary evaporator, **2q** was obtained as a white solid. The yield was 1.31 g (86%). $^1$H NMR (400 MHz, $CDCl_3$): $\delta$ 7.14 (dd, $J$ = 4.9 and 3.8 Hz, 1H), 7.66 (dd, $J$ = 4.9 and 1.3 Hz, 1H), 7.85 (dd, $J$ = 3.8 and 1.3 Hz, 1H).[9]

**[(PPh$_3$)$_2$Pd(Ph)N$_3$].** [(PPh$_3$)$_2$Pd(Ph)Br] (153 mg; 0.194 mmol) was added to a suspension of $NaN_3$ (252 mg; 3.9 mmol; 20 equiv) in MeOH (4 mL), and the mixture was sonicated for 1 h. Methanol (15 mL) was added and the liquid phase decanted off. To the solid residue were added $NaN_3$ (252 mg; 3.9 mmol; 20 equiv) and MeOH (4 mL), and the mixture was sonicated for 1 h. Again, MeOH (15 mL) was added, the solid was separated by decantation, and thoroughly extracted with warm (50 °C) benzene (3 × 5 mL). The benzene extract was filtered through a short Celite plug, concentrated to ca. 5 mL, and treated with hexanes (15 mL). After 12 h, the white precipitate was separated and dried under vacuum. The yield of [(PPh$_3$)$_2$Pd(Ph)N$_3$] was 129 mg (89%). This complex is air-stable in the solid state and in solution. Anal. Calcd for $C_{42}H_{35}N_3P_2Pd$: C, 67.3; H, 4.7; N, 5.6. Found: C, 67.2; H, 4.7; N, 5.6. $^1$H NMR ($CDCl_3$, 400 MHz): $\delta$ 6.29 (t, 2H, $J$ = 7.4 Hz, $C_6H_5Pd$), 6.43 (t, 1H, $J$ = 7.2 Hz, $C_6H_5Pd$), 6.62 (m, 2H, $C_6H_5Pd$), 7.24−7.33 (m, 12H, PPh$_3$), 7.33−7.44 (m, 18H, PPh$_3$). $^{31}$P NMR ($CDCl_3$, 162 MHz): $\delta$ 25.2 (s). IR (neat, cm$^{-1}$): 2043 ($N_3$). X-ray-quality crystals of *trans*-[(PPh$_3$)$_2$Pd(Ph)N$_3$] were obtained by slow diffusion of hexane into a concentrated solution of [(PPh$_3$)$_2$Pd(Ph)N$_3$] in chloroform in a 5 mm NMR tube. The complex crystallized in two polymorphic forms (white and yellow) displaying either a staggered or eclipsed conformation along the P−Pd−P axis, as shown in Figures 1 and 2.

**Reaction of [(PPh$_3$)$_2$Pd(Ph)N$_3$] with CO, PhI, and PPh$_3$.** Inside a glovebox, a mixture of [(PPh$_3$)$_2$Pd(Ph)N$_3$] (7 mg; 0.01 mmol), PPh$_3$ (5 mg; 0.02 mmol), PhI (50 $\mu$L), and benzene-$d_6$ (0.6 mL) was placed in a 5 mm NMR tube and sealed with a rubber septum. After CO was bubbled through this solution via a syringe needle and the tube was heated at 50 °C (oil bath) for 30 min, full conversion of [(PPh$_3$)$_2$Pd(Ph)N$_3$] to [(PPh$_3$)$_2$Pd(COPh)I] ($^{31}$P NMR: s, 18.8 ppm; lit.[6] 19.0 ppm) and PPh$_3$═NCOPh ($^{31}$P NMR: s, 20.8 ppm; lit.[12] 20.6 ppm) in a 1:1 molar ratio was observed.

**Preparation of [(Xantphos)PdI$_2$] (7).** A mixture of [(Xantphos)PdCl$_2$]·CH$_2$Cl$_2$ (**8**; 126 mg; 0.15 mmol), NaI (225 mg; 1.50 mmol), deionized water (2 mL), and CH$_2$Cl$_2$ (2 mL) was stirred in air for 30 min. The deep purple mixture was diluted with deionized water (5 mL) and CH$_2$Cl$_2$ (5 mL). The organic phase was separated and the aqueous phase was washed with CH$_2$Cl$_2$ (2 × 5 mL). The combined dichloromethane phase and the washings were dried over $Na_2SO_4$ and filtered through Celite. The filtrate was evaporated to ca. 5 mL, treated with Et$_2$O (25 mL), and kept at −32 °C overnight. The dark precipitate was separated, washed with Et$_2$O (2 × 5 mL), and dried under vacuum. The yield of **7** was 137 mg (97%). This complex is air-stable in the solid state and in solution. Anal. Calcd for $C_{39}H_{32}I_2OP_2Pd$: C, 49.9; H, 3.4. Found: C, 49.7; H, 3.7. For the VT $^1$H and $^{31}$P NMR data for **7**, see the Supporting Information. X-ray-quality single crystals of ***cis*-7**·CH$_2$Cl$_2$ were obtained by layering its solution (ca. 2 mg in 0.6 mL of CH$_2$Cl$_2$) with Et$_2$O (1 mL) and keeping the mixture at −32 °C for 3 days. X-ray-quality single crystals of ***trans*-7** were obtained by layering its solution (ca. 10 mg in 0.6 mL of CHCl$_3$) with Et$_2$O (1.6 mL) and keeping the mixture at −32 °C for 3 days (see Figure 3).

**Preparation of [(Xantphos)Pd(N$_3$)$_2$] (9).** Chloroform employed in this preparation was filtered through a short $K_2CO_3$ plug prior to use. A mixture of [(Xantphos)PdCl$_2$]·CH$_2$Cl$_2$ (**8**; 84 mg; 0.10 mmol), $NaN_3$ (130 mg; 2.0 mmol), deionized water (3 mL), and CHCl$_3$ (3 mL) was vigorously stirred in air for 30 min. The orange organic phase was separated and the aqueous phase was washed with CHCl$_3$ (2 × 3 mL). The combined chloroform phase and the washings were evaporated with a flow of argon to ca. 2 mL, treated with Et$_2$O (15 mL), and kept at +4 °C overnight. The orange needle crystals were separated, washed with Et$_2$O (2 × 3 mL), and dried under vacuum. The yield of **9** was 72 mg (94%). This complex is air-stable in the solid state and in solution. Anal. Calcd for $C_{39}H_{32}N_6OP_2Pd$: C, 60.9; H, 4.2; N, 10.9. Found: C, 60.5; H, 4.3; N, 10.7. $^1$H NMR ($CDCl_3$, 500 MHz): $\delta$ (for major isomer) 1.83 (s, 6H, 2CH$_3$), 7.12 (t, 8H, $J$ = 7.5 Hz), 7.19 (m, 2H), 7.25, (m, 6H), 7.31, (m, 8H), 7.68 (dd, $J$ = 7.8 and 1.1 Hz, 2H). $^{31}$P NMR ($CDCl_3$, 203 MHz): $\delta$ 7.7 (s, minor isomer, 5%), 21.3 (s, major isomer, 95%). IR (neat, cm$^{-1}$): 2018 ($N_3$). X-ray-quality single crystals of ***cis*-9**·CHCl$_3$ were obtained by slow evaporation of its CHCl$_3$ solution (Figure 4).

**Reaction of Pd$_2$(dba)$_5$ with Xantphos.** Inside a glovebox, a 5 mm NMR tube was charged with Pd$_2$(dba)$_5$ (7 mg; 0.01 mmol of Pd), Xantphos (6 mg; 0.01 mmol), and benzene-$d_6$ (0.6 mL) and sealed with a rubber septum. $^{31}$P NMR analysis of the sample showed complete conversion of Xantphos and the formation of two new species, [(Xantphos)Pd(dba)] (**11**; two doublets at 11.3 and 13.5 ppm, $J_{P-P}$ = 10.6 Hz) and [(Xantphos)$_2$Pd] (two broad multiplets at 3.5 and 6.0 ppm) in a 4:1 ratio. A similar $^{31}$P NMR pattern was observed for the reaction mixture obtained similarly using Pd$_2$(dba)$_5$ (28 mg; 0.04 mmol of Pd) and Xantphos (23 mg; 0.04 mmol) in THF (2 mL). After 1 week at room temperature, the THF solution produced X-ray-quality crystals of [(Xantphos)Pd(dba)]·3THF (**11**·3THF; see Figure 5).

**Reaction of Pd$_2$(dba)$_5$ with Xantphos and CO.** Inside a glovebox, a 5 mm NMR tube was charged with Pd$_2$(dba)$_5$ (7 mg; 0.01 mmol of Pd), Xantphos (6 mg; 0.01 mmol), and benzene-$d_6$ (0.6 mL) and sealed with a rubber septum. After the argon headspace was flushed with CO via a syringe needle, full conversion of the originally produced mixture of [XantphosPd(dba)] (**11**) and [(Xantphos)$_2$Pd] to [(Xantphos)Pd(CO)$_2$], (**12**; s, 10.5 ppm) was observed within 10 min ($^{31}$P NMR). Identical results were obtained when THF (0.6 mL) was used in place of benzene-$d_6$. Two strong bands at 1974 and 2014 cm$^{-1}$ were observed in the FT-IR spectrum of the solution (background subtraction).

**Reaction of [(Xantphos)Pd(Ph)I] (10) with CO.** Inside a glovebox, a 5 mm NMR tube was charged with [(Xantphos)Pd(Ph)I] (**10**; 7 mg; 0.008 mmol) and benzene-$d_6$ (0.5 mL) and sealed with a rubber septum. After the headspace was flushed with CO (syringe needle) for ca. 0.5 min, full conversion of **10** (s, 13.2 ppm) to [(Xantphos)Pd(COPh)I] (**13**; s, 3.2 ppm) was observed by $^{31}$P NMR.

**Reaction of [(Xantphos)Pd(CO)$_2$] (12) with PhI.** Inside a glovebox, a 5 mm NMR tube was charged with Pd$_2$(dba)$_5$ (7 mg; 0.01 mmol of Pd), Xantphos (6 mg; 0.01 mmol), and benzene-$d_6$ (0.6 mL) and sealed with a rubber septum. After the headspace was flushed with CO (syringe needle) for ca. 0.5 min, full conversion to [(Xantphos)Pd(CO)$_2$], (**12**; s, 10.5 ppm) was observed within 10 min ($^{31}$P NMR).

Addition of iodobenzene (20 $\mu$L) to the thus generated **12** resulted in selective formation of [(Xantphos)Pd(COPh)I] (**13**; $^{31}$P NMR: s, 3.2 ppm) at full conversion.

**Reaction of [(Xantphos)Pd(COPh)I] (13) with [Bu$_4$N]N$_3$.** Inside a glovebox, a 5 mm NMR tube was charged with [(Xantphos)Pd(Ph)I] (**10**; 7 mg; 0.008 mmol) and benzene-$d_6$ (0.5 mL) and sealed with a rubber septum. Replacing the argon headspace with CO (syringe needle) resulted in an instantaneous reaction leading to full conversion ($^{31}$P NMR) of **10** (s, 13.2 ppm[29]) to [(Xantphos)Pd(COPh)I] (**13**; s, 3.2 ppm). A solution of [Bu$_4$N]N$_3$ (10 mg; 0.035 mmol) in benzene-$d_6$ (0.2 mL) was added via syringe. The $^{31}$P NMR spectrum recorded within 10 min indicated full conversion of **13** to [(Xantphos)Pd(CO)$_2$] (**12**; s, 10.5 ppm). As the resultant solution of **12** and PhCON$_3$ was highly air-sensitive, the formation of the latter by IR was confirmed in a similar experiment performed in the presence of PhI (see below).

**Reaction of [(Xantphos)Pd(COPh)I] (13) with [Bu$_4$N]N$_3$ in the Presence of PhI.** Inside a glovebox, a 5 mm NMR tube was charged with Xantphos (6 mg; 0.01 mmol), Pd$_2$(dba)$_5$ (7 mg; 0.01 mmol of Pd), and benzene-$d_6$ (0.5 mL) and sealed with a rubber septum. The headspace was flushed with CO (syringe needle) for ca. 0.5 min. The addition of iodobenzene (20 $\mu$L) to the thus generated [(Xantphos)Pd(CO)$_2$] (**12**; see above) resulted in the selective formation of [(Xantphos)Pd(COPh)I] (**13**; $^{31}$P NMR: s, 3.2 ppm) at full conversion. To this sample was added via syringe 0.2 mL (1.2 equiv) of a solution of [Bu$_4$N]N$_3$ (34 mg) in C$_6$H$_6$ (2 mL). The FT-IR spectrum registered 10 min after the addition of azide indicated the formation of PhCON$_3$ (**2a**; neat, cm$^{-1}$): 2133 (N$_3$); 1695 (C═O) and no presence of PhNCO (2247 cm$^{-1}$). FT-IR for an authentic sample of **2a** (cm$^{-1}$): 2130 (N$_3$); 1691 (C═O).

**Reaction of [(Xantphos)Pd(Ph)I] (10) with [Bu$_4$N]N$_3$.** Inside a glovebox, a vial was charged with Xantphos (29 mg; 0.05 mmol), Pd$_2$(dba)$_5$ (35 mg; 0.05 mmol of Pd), PPh$_3$O (14 mg; 0.05 mmol; internal standard), and benzene (5 mL). After this reaction mixture was stirred for 1 min, PhI (100 $\mu$L) was added. $^{31}$P NMR analysis indicated full conversion of [(Xantphos)Pd(dba)] (**11**) to [(Xantphos)Pd(Ph)I] (**10**; s, 13.2 ppm) after 30 min. [Bu$_4$N]N$_3$ (16 mg; 0.06 mmol) was then added, and the solution was again analyzed by $^{31}$P NMR after 10 min to observe full conversion to [(Xantphos)Pd(Ph)N$_3$] (**14**; s, 11.0 ppm).

**Reaction of [(Xantphos)Pd(Ph)I] (10) with NaN$_3$.** Inside a glovebox, a vial was charged with Xantphos (29 mg; 0.05 mmol), Pd$_2$(dba)$_5$ (35 mg; 0.05 mmol of Pd), PPh$_3$O (14 mg; 0.05 mmol; internal standard), and benzene (5 mL). After the mixture was stirred for 1 min, PhI (100 $\mu$L) was added. $^{31}$P NMR analysis after 30 min indicated full conversion of [(Xantphos)Pd(dba)] (**11**) to [(Xantphos)Pd(Ph)I] (**10**; s, 13.2 ppm). Argon-saturated water (5 mL) and sodium azide (32 mg; 0.5 mmol) were added. After 5 min of vigorous agitation, a 0.2 mL aliquot of the organic layer was diluted with C$_6$H$_6$ (1 mL) and analyzed by $^{31}$P NMR (IGD) to show ca. 60% conversion to [(Xantphos)Pd(Ph)N$_3$] (**14**; s, 11.0 ppm). No change in the composition of the organic layer was observed ($^{31}$P NMR) after stirring the biphasic system for an additional 1 h.

**Reaction of [(Xantphos)Pd(Ph)N$_3$] (14) with CO.** Inside a glovebox, a 5 mm NMR tube was charged with **14** (7 mg; 0.01 mmol) and toluene (0.6 mL) and sealed with a rubber septum. After the mixture was placed under CO by purging via a syringe needle for ca. 0.5 min, full conversion of **14** to [(Xantphos)Pd(CO)$_2$] (**12**; s, 10.5 ppm) was observed within 10 min ($^{31}$P NMR). Layering the resultant solution with hexanes under CO produced X-ray-quality crystals of [(Xantphos)Pd(CO)$_2$]·$n$-C$_6$H$_{14}$ (**12**·hexane; see Figure 6).

**Reaction of [(Xantphos)Pd(Ph)N$_3$] (14) with CO in the Presence of PhI.** Inside a glovebox, a 5 mm NMR tube was charged with **14** (7 mg; 0.01 mmol), PhI (20 $\mu$L), and benzene-$d_6$ (0.6 mL) and sealed with a rubber septum. After the reaction mixture was placed under a CO atmosphere by purging via a syringe needle for ca. 0.5 min, full conversion of **14** to [(Xantphos)Pd(COPh)I] (**13**; $^{31}$P NMR s, 3.2 ppm) was observed within 10 min by $^{31}$P NMR. The formation of PhCON$_3$ (**2a**) was confirmed by FT-IR (neat, cm$^{-1}$): 2133 (N$_3$); 1694 (C═O). FT-IR for independently prepared and isolated **2a** (neat, cm$^{-1}$): 2130 (N$_3$); 1691 (C═O). No characteristic band from NCO was observed (2247 cm$^{-1}$ for an authentic sample of PhNCO).

**[Bu$_4$N]N$_3$.** A 50% aqueous solution of tetra-$n$-butylammonium sulfate (5.8 g; 5.0 mmol of [NBu$_4$]$_2$SO$_4$) was concentrated on a rotary evaporator. After a total of 2.1 g of water had been evaporated, NaN$_3$ (1.95 g; 30 mmol) was added and the resultant mixture was agitated for 20 h. Acetonitrile (30 mL) and anhydrous sodium sulfate (10 g) were added, and the mixture was stirred for 30 min and filtered. The solid on the filter was washed with acetonitrile (2 × 10 mL). The combined filtrate and the washings were evaporated on a rotary evaporator. Drying the residue under vacuum (ca. 1 mmHg) overnight produced a white solid (2.88 g). The thus obtained crude [Bu$_4$N]N$_3$ was brought to a glovebox and dissolved in dry benzene (20 mL). The resultant solution was filtered through a pad of Celite. The reaction flask was rinsed with dry benzene (2 × 10 mL) and the washings were filtered through the same pad. The combined filtrate and the washings were evaporated and dried under vacuum at ca. 1 mmHg for 20 h. Trituration of the residue with dry ether (40 mL) produced a white crystalline solid that was separated and dried under vacuum (ca. 1 mmHg) for 20 h. The yield of [Bu$_4$N]N$_3$ was 2.79 g (98%). This salt is hygroscopic and was therefore stored and used in a glovebox. $^1$H NMR (500 MHz, CDCl$_3$): $\delta$ 1.00 (t, $J$ = 7.4 Hz, 3H), 1.45 (tq, $J$ = 7.4 and 7.4 Hz, 2H), 1.68 (m, 2H), 3.35 (m, 2H). IR (neat, cm$^{-1}$): 1991 (N$_3^-$). X-ray-quality single crystals of [Bu$_4$N]N$_3$·C$_6$H$_6$ were obtained from a concentrated benzene solution on standing at room temperature (Figure 13).

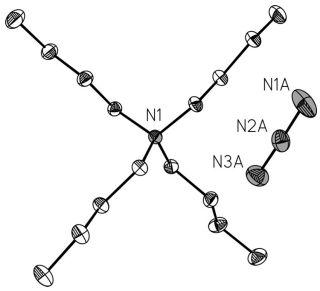


**Figure 13.** ORTEP drawing of [Bu$_4$N]N$_3$·C$_6$H$_6$ with benzene and all H atoms omitted and thermal ellipsoids drawn at the 50% probability level.

**Computational Details.** Calculations were run with Gaussian 03 Revision D.01[58] with PCM solvent corrections run with Gaussian 09 Revision A.02.[59] Geometry optimizations were performed using the BP86 functional[60] and employed a smaller basis set, BS1, in which the Pd, P, and I centers were described with the Stuttgart RECPs and associated basis sets[61] (with added d-orbital polarization on P ($\zeta$ = 0.387) and I ($\zeta$ = 0.289)[62]) and 6-31G** basis sets for all other atoms. All stationary points were fully characterized via analytical frequency calculations as either minima (all positive eigenvalues) or transition states (one negative eigenvalue) and IRC calculations, and subsequent geometry optimizations were used to confirm the minima linked by each transition state. Frequency calculations also provided a free energy in the gas phase, computed at 298.15 K and 1 atm. As has been found by others,[63] reasonable barriers, in particular for the initial oxidative addition steps, required a correction for dispersion effects to be included and this was obtained via a single-point energy calculation on the BP86(BS1)-optimized geometries using Grimme's D3 parameter set[64] (i.e., BP86-D3). Moreover, the energetics of I$^-$/N$_3^-$ exchange were found to be highly sensitive to the choice of basis set, this process being unrealistically exergonic with BS1 that was used in the geometry optimization. All energies were therefore recomputed with a larger basis set, BS2, featuring aug-CC-pVTZ on Pd, P, and I and 6-311++G** on all other atoms. Further details on this basis set dependency are given in Table S5 in the Supporting Information for I$^-$/N$_3^-$ exchange at ***trans*-10** and ***cis*-13**. Starting geometries for the various minima were taken from experimental crystallographic studies (e.g., for **11**, **12**, ***cis*-13**, ***trans*-14**) reported here, as well as for ***trans***-

**10**[29] or by adapting these structures (e.g., via replacement of $I^-$ by $N_3^-$). Computed geometries reproduced the available experimental data well (see Table S4 in the Supporting Information). A number of different conformations were tested for each stationary point, and in particular the transition states $\mathbf{TS_{RC}}$, $\mathbf{TS_{MI}(I)}$, $\mathbf{TS_{OA1}}$, and $\mathbf{TS_{OA2}}$ were subject to extensive conformational searching using our published protocol.[65]

## ■ ASSOCIATED CONTENT

### Supporting Information

Text, tables, figures, and CIF files giving full details of experimental, computational, and crystallographic studies, including full refs 58 and 59. This material is available free of charge via the Internet at http://pubs.acs.org.

## ■ AUTHOR INFORMATION


### Corresponding Authors

*E-mail for S.A.M.: s.a.macgregor@hw.ac.uk.

*E-mail for V.V.G.: vgrushin@iciq.es.


### Notes

The authors declare no competing financial interest.

## ■ ACKNOWLEDGMENTS

The ICIQ Foundation, Consolider Ingenio 2010 (Grant CSD2006-0003), and The Spanish Government (Grant CTQ2011-25418) are thankfully acknowledged for support of this work. S.A.M. and C.L.M. thank the EPSRC for support through award EP/J021911/1.

## ■ REFERENCES


(1) (a) Schoenberg, A.; Bartoletti, I.; Heck, R. F. *J. Org. Chem.* **1974**, *39*, 3318. (b) Schoenberg, A.; Heck, R. F. *J. Org. Chem.* **1974**, *39*, 3327. (c) Schoenberg, A.; Heck, R. F. *J. Am. Chem. Soc.* **1974**, *96*, 7761.

(2) For recent reviews on Pd-catalyzed carbonylation reactions of aryl halides, see: (a) Wu, X.-F.; Neumann, H.; Beller, M. *Chem. Rev.* **2013**, *113*, 1. (b) Roy, S.; Roy, S.; Gribble, G. W. *Tetrahedron* **2012**, *68*, 9867. (c) Wu, X.-F.; Neumann, H.; Beller, M. *Chem. Soc. Rev.* **2011**, *40*, 4986. (d) Magano, J.; Dunetz, J. R. *Chem. Rev.* **2011**, *111*, 2177. (e) Grigg, R.; Mutton, S. P. *Tetrahedron* **2010**, *66*, 5515. (f) Brennführer, A.; Neumann, H.; Beller, M. *Angew. Chem., Int. Ed.* **2009**, *48*, 4114. (g) Barnard, C. F. J. *Organometallics* **2008**, *27*, 5402.

(3) For general reviews, see: (a) Scriven, E. F. V.; Turnbull, K. *Chem. Rev.* **1988**, *88*, 297. (b) Bräse, S.; Gil, C.; Knepper, K.; Zimmermann, V. *Angew. Chem., Int. Ed.* **2005**, *44*, 5188. (c) Bräse, S.; Banert, K. *Organic Azides: Syntheses and Applications*; Wiley: Chichester, U.K., 2010.

(4) Cano, I.; Álvarez, E.; Nicasio, M. C.; Pérez, P. J. *J. Am. Chem. Soc.* **2011**, *133*, 191.

(5) Katritzky, A. R.; Widyan, K.; Kirichenko, K. *J. Org. Chem.* **2007**, *72*, 5802.

(6) Garrou, P. E.; Heck, R. F. *J. Am. Chem. Soc.* **1976**, *98*, 4115.

(7) Kim, Y.-J.; Kwak, Y.-S.; Lee, S.-W. *J. Organomet. Chem.* **2000**, *603*, 152.

(8) For a recent review of the Staudinger reaction, see: Iula, D. M. In *Name Reactions for Functional Group Transformations*; Li, J. J., Corey, E. J., Eds.; Wiley: Hoboken, NJ, 2007; p 129.

(9) Miloserdov, F. M.; Grushin, V. V. *Angew. Chem., Int. Ed.* **2012**, *51*, 3668.

(10) Barluenga, J.; Valdés, C.; Beltrán, G.; Escribano, M.; Aznar, F. *Angew. Chem., Int. Ed.* **2006**, *45*, 6893.

(11) For selected examples of the facile formation of various organopalladium azido complexes from the corresponding Pd(II) halides and $NaN_3$, see: (a) Kim, Y.-J.; Choi, J.-C.; Park, K.-H. *Bull. Korean Chem. Soc.* **1994**, *15*, 690. (b) Kim, Y.-J.; Kim, D.-H.; Song, S.-W.; Son, T.-i. *Bull. Korean Chem. Soc.* **1998**, *19*, 125. (c) Kim, Y.-J.; Chang, X.; Han, J.-T.; Lim, M. S.; Lee, S. W. *Dalton Trans.* **2004**, 3699. (d) Lee, K.-E.; Jeon, H.-T.; Han, S.-Y.; Ham, J.; Kim, Y.-J.; Lee, S. W. *Dalton Trans.* **2009**, 6578.

(12) Albright, T. A.; Freeman, W. J.; Schweizer, E. E. *J. Org. Chem.* **1976**, *41*, 2716.

(13) (a) The empirical composition $Pd_2(dba)_5$ was derived from elemental analysis data.[13b] (b) Ushkov, A. V.; Grushin, V. V. *J. Am. Chem. Soc.* **2011**, *133*, 10999.

(14) For selected reviews on Xantphos and related ligands, see: (a) Kamer, P. C. J.; Van Leeuwen, P. W. N. M.; Reek, J. N. H. *Acc. Chem. Res.* **2001**, *34*, 895. (b) Freixa, Z.; Van Leeuwen, P. W. N. M. *Dalton Trans.* **2003**, 1890. (c) Freixa, Z.; Van Leeuwen, P. W. N. M. *Coord. Chem. Rev.* **2008**, *252*, 1755. (d) Van Leeuwen, P. W. N. M.; Freixa, Z. In *Modern Carbonylation Methods*; Kollar, L., Ed.; Wiley-VCH: Weinheim, Germany, 2008; p 1.

(15) For efficient catalysis of other carbonylation reactions with Xantphos/Pd, see: (a) Martinelli, J. R.; Watson, D. A.; Freckmann, D. M. M.; Barder, T. E.; Buchwald, S. L. *J. Org. Chem.* **2008**, *73*, 7102. (b) Ueda, T.; Konishi, H.; Manabe, K. *Org. Lett.* **2013**, *15*, 5370.

(16) In the ligand screening experiments, GC-MS was used for analysis, which could not allow for direct detection of $PhCON_3$ because of its instantaneous Curtius rearrangement in the GC injector. The conversions and yields were therefore derived from the quantities of PhNCO observed.

(17) Klingensmith, L. M.; Strieter, E. R.; Barder, T. E.; Buchwald, S. L. *Organometallics* **2006**, *25*, 82.

(18) (a) Shen, Q.; Ogata, T.; Hartwig, J. F. *J. Am. Chem. Soc.* **2008**, *130*, 6586. (b) Fors, B. P.; Davis, N. R.; Buchwald, S. L. *J. Am. Chem. Soc.* **2009**, *131*, 5766.

(19) It was established in a separate experiment that $NaN_3$ in excess does not deactivate the catalyst.

(20) Saikachi, H.; Kitagawa, T.; Nasu, A.; Sasaki, H. *Chem. Pharm. Bull.* **1981**, *29*, 237.

(21) (a) Bertani, R.; Berton, A.; Di Bianca, F.; Crociani, B. *J. Organomet. Chem.* **1986**, *303*, 283. (b) Isobe, K.; Nanjo, K.; Nakamura, Y.; Kawaguchi, S. *Bull. Chem. Soc. Jpn.* **1986**, *59*, 2141.

(22) Yukawa, Y.; Tsuno, Y. *J. Am. Chem. Soc.* **1958**, *80*, 6346.

(23) Wu, X.-F.; Neumann, H.; Beller, M. *Chem. Eur. J.* **2010**, *16*, 9750.

(24) Ulrich, H. *Chemistry and Technology of Isocyanates*; Wiley: Chichester, U.K., 1997.

(25) Tkatchenko, I.; Jaouhari, R.; Bonnet, M.; Dawkins, G.; Lecolier, S. U.S. Patent 4749806, 1987.

(26) (a) Vinogradova, E. V.; Fors, B. P.; Buchwald, S. L. *J. Am. Chem. Soc.* **2012**, *134*, 11132. (b) Vinogradova, E. V.; Park, N. H.; Fors, B. P.; Buchwald, S. L. *Org. Lett.* **2013**, *15*, 1394.

(27) Erhardt, S.; Grushin, V. V.; Kilpatrick, A. H.; Macgregor, S. A.; Marshall, W. J.; Roe, D. C. *J. Am. Chem. Soc.* **2008**, *130*, 4828.

(28) Under identical conditions (10 mmol of PhI in 0.5 mL of THF) with **7** (0.2 mol %) as added catalyst at room temperature, the reaction stopped after 2 h at ca. 20% conversion.

(29) Grushin, V. V.; Marshall, W. J. *J. Am. Chem. Soc.* **2006**, *128*, 12644.

(30) Bakhmutov, V. I.; Bozoglian, F.; Gómez, K.; González, G.; Grushin, V. V.; Macgregor, S. A.; Martin, E.; Miloserdov, F. M.; Novikov, M. A.; Panetier, J. A.; Romashov, L. V. *Organometallics* **2012**, *31*, 1315.

(31) See, for example: (a) Redfield, D. A.; Nelson, J. H. *Inorg. Chem.* **1973**, *12*, 15. (b) Anderson, G. K.; Cross, R. J. *Chem. Soc. Rev.* **1980**, *9*, 185.

(32) Grushin, V. V. *Chem. Rev.* **2004**, *104*, 1629.

(33) In the presence of larger quantities of PMHS (2 equiv) at 50 °C, the aroyl azide product undergoes reduction to the corresponding benzamide (see above).

(34) Ozawa, F.; Soyama, H.; Yanagihara, H.; Aoyama, I.; Takino, H.; Izawa, K.; Yamamoto, T.; Yamamoto, A. *J. Am. Chem. Soc.* **1985**, *107*, 3235.

(35) (a) Mägerlein, W.; Beller, M.; Indolese, A. F. *J. Mol. Catal. A: Chem.* **2000**, *156*, 213. (b) Gaviño, R.; Pellegrini, S.; Castanet, Y.; Mortreux, A.; Mentré, O. *Appl. Catal., A* **2001**, *217*, 91.

(36) See footnote 77 in Kolb, H. C.; Finn, M. G.; Sharpless, K. B. *Angew. Chem., Int. Ed.* **2001**, *40*, 2004.
(37) González-Bobes, F.; Kopp, N.; Li, L.; Deerberg, J.; Sharma, P.; Leung, S.; Davies, M.; Bush, J.; Hamm, J.; Hrytsak, M. *Org. Process Res. Dev.* **2012**, *16*, 2051 and references cited therein.
(38) (a) Beck, W.; Fehlhammer, W. P.; Pöllmann, P.; Schuierer, E.; Feldl, K. *Chem. Ber.* **1967**, *100*, 2335. (b) Beck, W.; Klapötke, T. M.; Knizek, J.; Nöth, H.; Schütt, T. *Eur. J. Inorg. Chem.* **1999**, 523.
(39) Reported mechanistic information on oxidative addition of organic halides to mixed phosphino carbonyl Pd(0) species is extremely limited. For selected examples, see: (a) Kudo, K.; Sato, M.; Hidai, M.; Uchida, Y. *Bull. Chem. Soc. Jpn.* **1973**, *46*, 2820. (b) Stille, J. K.; Lau, K. S. Y. *J. Am. Chem. Soc.* **1976**, *98*, 5841. (c) Lau, K. S. Y.; Wong, P. K.; Stille, J. K. *J. Am. Chem. Soc.* **1976**, *98*, 5832.
(40) Braterman, P. S. *Metal Carbonyl Spectra*; Academic Press: London, 1975.
(41) Gjaldbæk, J. Chr. *Acta Chem. Scand.* **1952**, *6*, 623.
(42) X-ray-quality crystals of tetrabutylammonium azide formed from its benzene solution on standing. One of them was used for the crystal structure determination of $[Bu_4N]^+N_3^-$ (see the Experimental Section and the Supporting Information for details).
(43) Fujita, K.; Yamashita, M.; Puschmann, F.; Martinez Alvarez-Falcon, M.; Incarvito, C. D.; Hartwig, J. F. *J. Am. Chem. Soc.* **2006**, *128*, 9044.
(44) (a) Grushin, V. V. *Angew. Chem., Int. Ed.* **1998**, *37*, 994. (b) Flemming, J. P.; Pilon, M. C.; Borbulevitch, O. Ya.; Antipin, M. Yu.; Grushin, V. V. *Inorg. Chim. Acta* **1998**, *280*, 87.
(45) Coyle, R. J.; Slovokhotov, Yu. L.; Antipin, M. Yu.; Grushin, V. V. *Polyhedron* **1998**, *17*, 3059.
(46) For previous computational studies of Ph−X activation (X = Cl, Br) at [Pd(Xantphos)], see: Hicks, J. D.; Hyde, A. M.; Cuezva, A. M.; Buchwald, S. L. *J. Am. Chem. Soc.* **2009**, *131*, 16720. Structure **2a** reported in that work is related to **I3** located here, although in that case no Pd−O interaction was apparent and a different orientation of the Ph ligand was seen.
(47) Alternative isomers of **I4(I)** are possible, e.g., with CO trans to phosphine and Ph trans to I. However, migratory insertion has been shown to be facilitated when the transferring group (here Ph) is trans to a highest trans influence coligand, i.e., as in **I4(I)**, in which Ph is trans to phosphine. For a related example, see: Macgregor, S. A.; Neave, G. W. *Organometallics* **2004**, *23*, 891.
(48) We have not attempted to locate transition states for $I^-/N_3^-$ exchange but have assumed that this readily occurs under the reaction conditions, as was shown to be the case experimentally for the conversion of **10** to **14**.
(49) We also attempted to locate a pathway for C−N bond formation via the direct nucleophilic attack of free azide at the benzoyl ligand in **15**. Several linear transits were run to probe this possibility, with optimizations being run with the water solvent being included in the SCF procedure in order to treat the free anionic nucleophile. However, in all cases the approach of azide led to facile formation of a Pd−$N_3$ bond (with displacement of iodide or one arm of the Xantphos ligand) prior to C−N bond formation.
(50) (a) Fitton, P.; McKeon, J. E. *Chem. Commun.* **1968**, 4. (b) Fitton, P.; Johnson, M. P.; McKeon, J. E. *Chem. Commun.* **1968**, 6. (c) Fitton, P.; Rick, E. A. *J. Organomet. Chem.* **1971**, *28*, 287.
(51) Hartwig, J. *Organotransition Metal Chemistry: From Bonding to Catalysis*; University Science Books: Sausalito, CA, 2010.
(52) As described above, upon addition of 1 equiv of $[Bu_4N]N_3$ to [(Xantphos)Pd(Ph)(I)] (**10**) in benzene [(Xantphos)Pd(Ph)($N_3$)] (**14**) is formed quantitatively ($^{31}$P NMR). This, translates into **14**:**10** > 100, considering the sensitivity of the method (ca. 1%).
(53) Huser, M.; Youinou, M.-T.; Osborn, J. A. *Angew. Chem., Int. Ed. Engl.* **1989**, *28*, 1386.
(54) For a general review of $^{11}$C labeling, see: Antoni, G.; Kihlberg, T.; Långström, B. In *Handbook of Nuclear Chemistry*, 2nd ed.; Vértes, A., Nagy, S., Klencsár, Z., Lovas, R. G., Rösch, F., Eds.; Springer: Dordrecht, The Netherlands, 2011; Vol. *4*, p 1977.
(55) For recent examples of Pd-catalyzed carbonylation reactions with $^{11}$CO, see: (a) Kealey, S.; Plisson, C.; Collier, T. L.; Long, N. J.; Husbands, S. M.; Martarello, L.; Gee, A. D. *Org. Biomol. Chem.* **2011**, *9*, 3313. (b) Eriksson, J.; van den Hoek, J.; Windhorst, A. D. *J. Labelled Compd. Radiopharm.* **2012**, *55*, 223. (c) Takashima-Hirano, M.; Ishii, H.; Suzuki, M. *ACS Med. Chem. Lett.* **2012**, *3*, 804. (d) Dahl, K.; Schou, M.; Amini, N.; Halldin, C. *Eur. J. Org. Chem.* **2013**, 1228.
(56) Grushin, V. V. *Organometallics* **2000**, *19*, 1888.
(57) Johns, A. M.; Utsunomiya, M.; Incarvito, C. D.; Hartwig, J. F. *J. Am. Chem. Soc.* **2006**, *128*, 1828.
(58) Frisch, M. J., et al. *Gaussian 03, Revision D.01*; Gaussian Inc., Wallingford, CT, 2004.
(59) Frisch, M. J., et al. *Gaussian 09, Revision A.02*; Gaussian Inc., Wallingford, CT, 2009.
(60) (a) Becke, A. D. *Phys. Rev. A* **1988**, *38*, 3098. (b) Perdew, J. P. *Phys. Rev. B* **1986**, *33*, 8822.
(61) Andrae, D.; Häußermann, U.; Dolg, M.; Stoll, H.; Preuß, H. *Theor. Chim. Acta* **1990**, *77*, 123.
(62) Höllwarth, A.; Böhme, M.; Dapprich, S.; Ehlers, A. W.; Gobbi, A.; Jonas, V.; Köhler, K. F.; Stegmann, R.; Veldkamp, A.; Frenking, G. *Chem. Phys. Lett.* **1993**, *208*, 237.
(63) McMullin, C. L.; Jover, J.; Harvey, J. N.; Fey, N. *Dalton Trans.* **2010**, *39*, 10833.
(64) Grimme, S.; Antony, J.; Ehrlich, S.; Krieg, H. *J. Chem. Phys.* **2010**, *132*, 154104.
(65) Häller, L. J. L.; Page, M. J.; Erhardt, S.; Macgregor, S. A.; Mahon, M. F.; Naser, M. A.; Velez, A.; Whittlesey, M. K. *J. Am. Chem. Soc.* **2010**, *132*, 18408.